Nanoparticle Clearance from the Airways

Development and Testing of a New *In Vitro* Model to Investigate Mucociliary Clearance of Aerosol Particles

Dissertation
zur Erlangung des Grades
des Doktors der Naturwissenschaften
der Naturwissenschaftlich-Technischen Fakultät III
Chemie, Pharmazie, Bio- und Werkstoffwissenschaften
der Universität des Saarlandes

von

Andreas Michael Henning

Saarbrücken
2008

Tag des Kolloquiums:	12. Dezember, 2008
Dekan:	Prof. Dr. Uli Müller
Vorsitzender:	Prof: Dr. Hans H. Maurer
1. Gutachter:	Prof. Dr. Claus-Michael Lehr
2. Gutachter:	Prof. Dr. Elmar Heinzle
Akad. Mitarbeiter:	Dr. Michael Bur

Table of Contents

1. Summary

The current challenge in pulmonary drug delivery is to overcome and to control drug clearance from the lung. Here, the interaction with the mucociliary lung clearance plays a key role for any drug formulation technology. By today many open questions on mucociliary clearance (MC) have to be answered but suffer from limited experimental options. Considering these facts, the central part of this work was to develop a new *in vitro* test model to investigate the complex mechanism of MC more detailed. In a next step the new model was employed to study the influence of different factors on mucociliary particle clearance. From the overall results it can be concluded that:

- A new embryonic chicken trachea-based *in vitro* model to study MC was successfully developed and characterized.
- The model exhibits a stability and sensitivity for environmental as well as chemical influences reflecting the *in vivo* situation.
- Size and ζ-potential (ZP) seem to be minor critical factors for mucociliary particle clearance, which could be shown for different polymeric particles covering a broad size and ZP range.
- The chemical surface structure of nanoparticles was found to be a most relevant factor for MC, offering promising possibilities to achieve faster or slower particle transport.

In summary, this model may help to clarify open questions on lung clearance, strongly limiting the benefit of pulmonary drug delivery, and to realize the '3R' concept in animal testing: *Reduce, Refine, and Replace.*

2. Zusammenfassung

Die kontrollierte Arzneistoffelimination aus der Lunge stellt für die Inhalative Therapie eine große Herausforderung dar. Von zentraler Bedeutung, doch bis heute mit vielen offenen Fragen verbunden, ist hierbei die mukoziliäre Clearance (MC). Ziel dieser Arbeit war daher die Entwicklung eines neuen *in vitro* Modells für die gezielte Untersuchung mukoziliärer Transportprozesse sowie die anschließende Testung verschiedener Einflussfaktoren auf die MC von Partikeln. Aufgrund der Ergebnisse dieser Arbeit können folgende Schlüsse gezogen werden:

- Ein auf embryonaler Hühnertrachea basierendes *in vitro* Testsystem zur Untersuchung der MC wurde erfolgreich entwickelt und charakterisiert.
- Das Modell weist gegenüber äußeren Einflüssen und Arzneistoffen eine mit der *in vivo* Situation vergleichbare Stabilität sowie Sensitivität auf.
- Partikelgröße sowie ζ-Potenzial scheinen für die MC von untergeordneter Bedeutung zu sein, was für verschiedene Polymerpartikel unterschiedlicher Ladung und Größe gezeigt werden konnte.
- Die chemische Struktur und Oberflächenbeschaffenheit nanoskaliger Partikel scheint ein wichtiger Parameter für die MC zu sein und stellt damit einen Erfolg versprechenden Ansatz für die kontrollierte Arzneistoffelimination aus der Lunge dar.

Zusammenfassend besteht mit diesem neuen *in vitro* Modell künftig die Option, mukoziliäre Transportprozesse unter Beachtung des 3R-Konzepts für Tierexperimente (*Reduce, Refine, and Replace*) gezielt zu untersuchen und aufzuklären.

3. General Introduction

Parts of this chapter will be published in:

Henning A., Hein S., Schneider M., Bur M., Lehr C.-M. (2009): *Aerosol Delivery: Inhaling Medicines*. In: Handbook of Experimental Pharmacology: Novel Drug Delivery Approaches; Eds. Hofmann F., Schaefer-Korting M.S., Springer, New York, USA.

3.1. Inhalation in History

Already several thousand years ago mankind has been employing the respiratory route for drug delivery purposes. Ancient Egyptian physicians used the energy of hot stones to evaporate alkaloids from plants in order to make their patients inhale the active substances (Sanders, 2007). Indian as well as Native American shamans knew about the anti-asthmatic effects of *Datura stramonium* when leaves were smoked in a pipe or simply burned within a small room (Dessanges, 2001). Moreover, the smoking of opium, containing highly analgesic alkaloids from *Papaver somniferum*, has a long tradition in Chinese culture, although the medical aspect was not of primary relevance in this case. Hence, it is not surprising that in the course of time inhalation technology as well as the general knowledge of therapeutic inhalation continuously developed, and by today still is. In order to make inhalation more effective, the simple smoking pipes from the beginning were soon replaced by more ingenious inhalation instruments (Figure 1).

Figure 1: Historical Inhalation Devices

Left image: Smoking pipe found at Lake Valencia, in Venezuela. This pipe dates from about 800 BC to 1200 AD. Cave drawings from this period and region also depict pipes being smoked. *Right image:* The 'Pneumostat' was a very early compressor nebulizer manufactured by Weil in Frankfurt in the early 1930's. The 'Pneumostat' was used to deliver doses of Bronchovydrin (papaverin and eumydrine). By courtesy of Mark Sanders.

It was already in 1654 when the first illustration of an inhaler was depicted in Christopher Bennet's *Theatri Tabidorum* (Bennet, 1654). However, the term "inhaler" was introduced in 1778 by John Mudge, an English physician giving advice to treat cough via inhalation of opium vapor (Mudge, 1778). Accompanied by the continuous technical optimization, the improved understanding of pulmonary drug delivery principles also mediated a more defined and accurate vocabulary in this field. According to Aiache, it were R. Whitlaw and E. Gray Patterson who defined the word "aerosol" in 1932, based on "aer" (air) and "sol" (solution) (Aiache, 1990). Hitherto, the terms "mist", "micromist", "fog", and "fume" were used in an imprecise and often even confusing manner. This is astonishing from a current view of things, as a defined vocabulary is one of the fundamental requirements in every field of today's science.

The driving force to improve medical inhalation, especially in the 19th century, was the treatment of Consumption or pulmonary phthisis, whereas today the focus is given more in the treatment of asthma, COPD (Chronic obstructive pulmonary disease), and cystic fibrosis (CF) therapy. Till today this development results in a continuously increasing number of approved inhalation products as well as new therapeutic approaches, such as vaccination via the pulmonary route (Bivas-Benita et al., 2005; Lu and Hickey, 2007) and highly specific lung lobe targeting (Selting et al., 2008).

With regard to the current status, several respiratory diseases can be adequately treated by inhalation therapy (Groneberg et al., 2003). For many asthma and COPD patients, drug inhalation is even suitable to serve as the only form of therapeutic intervention. This in fact offers an important advantage regarding the patient's compliance and overall benefit from the therapy. Though, depending on the actual status and general severity of the disease, drug inhalation is needed once or several times per day. It is of particular importance to note that the correct drug application, here inhalation maneuver, results in a superior therapeutic effect and consequently a lower application rate (Booker, 2005; Serra-Batlles et al., 2002; Welch et al., 2004).

Due to this fact every patient receiving inhalative medication should be thoroughly trained in order to optimize drug deposition within the respiratory tract. However, in most cases it is rather the suboptimal inhalation technique than other factors, e.g. the lungs efficient clearance mechanisms, significantly limiting the success of the therapeutic regimen.

3.2. Lung Structure and Resulting Opportunities

Against the background of a continuously growing medical interest in pulmonary drug delivery, the gentle reader may already have scrutinized the scientific and economic reasons for this development. First and foremost it is the extremely thin (0.1 -0.5 µm) air-blood barrier (Figure 2) and the huge surface area of the lung (~140m^2) which predominantly contribute to the lungs unique and promising barrier properties for pharmaceutical drug delivery.

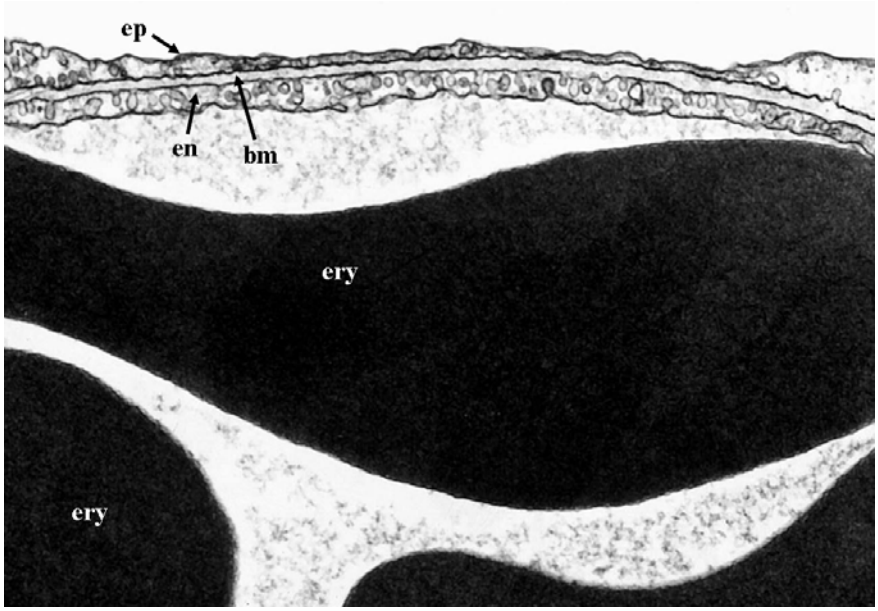

Figure 2: The Air-Blood Barrier

The TEM image (cross section) shows the epithelium (ep), the endothelium (en), the basal membrane (bm), and erythrocytes (ery) within an alveolar capillary. By courtesy of Peter Gehr, Institute of Anatomy, University of Bern, Bern, Switzerland.

Considering overall morphology of the lung, the organ consists of at least two dissimilar zones: the centrally located *conducting airways*, and the peripherally located *respiratory zone*. More precisely, the trachea, the main bronchi, and the conducting bronchioles account for the *conducting airways*, whereas the respiratory bronchioles, alveolar ducts, and the alveoli account for the lung's *respiratory zone* (Figure 3). Based on the tree-like branching pattern, the lung's structure is commonly subdivided into particular airway generations, starting with the trachea as generation 0, and ending with the alveoli as generation 23 (Albertine et al., 2000).

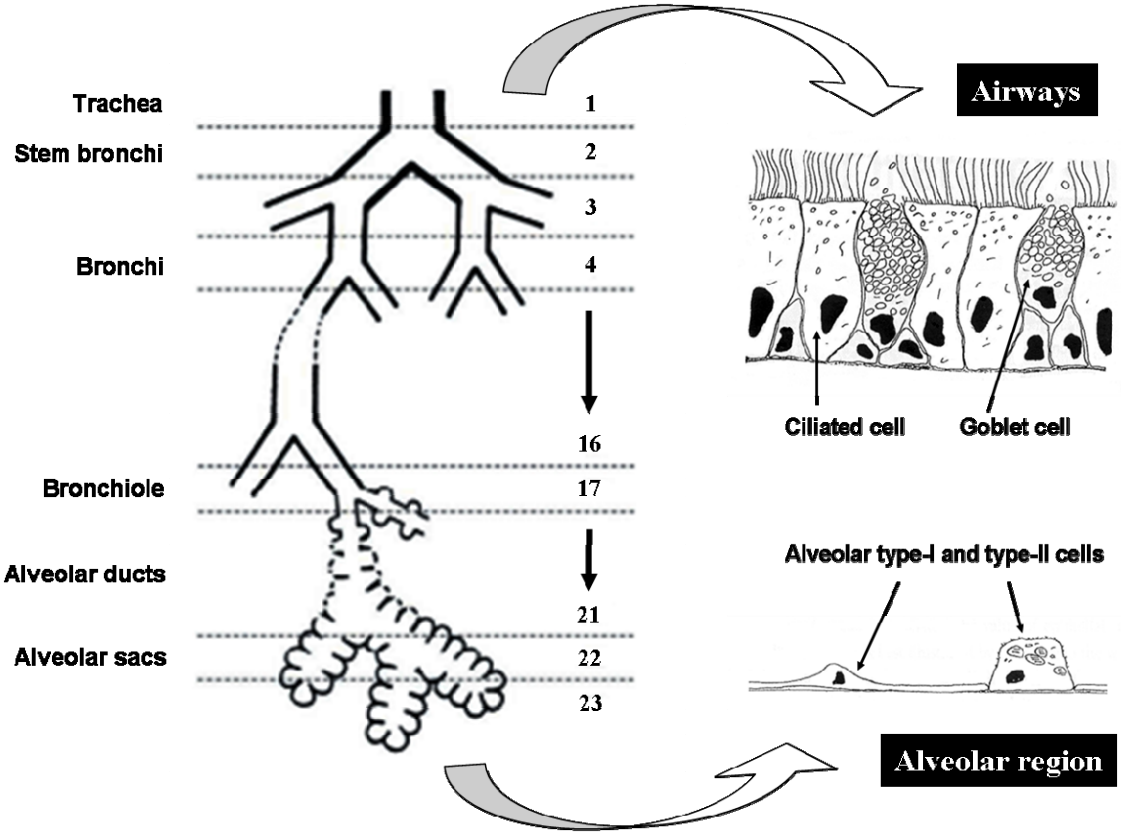

Figure 3: Schematic Lung Structure

Left: Human airway structure exhibits symmetric branching from the trachea to the alveolar region. *Right:* In the upper airways a columnar epithelium mainly consisting of ciliated cells and goblet cells is found, whereas in the alveolar region a flat and monolayer epithelium is formed by alveolar type-I and type-II cells.

As might be already assumed from the terminology, the conducting airways' function is mainly limited to air bulk flow during the active in- and exhaling process, whereas the essential and to the lungs designated gas-exchange function is exclusively realized within the respiratory zone. With regard to the lung epithelium, significant changes are present comparing the columnar, ciliated epithelium of the upper airways and the monolayer, non-ciliated epithelium of the alveolar region (Forbes, 2002; Forbes and Ehrhardt, 2005).

This unique morphological situation, namely the thin and huge alveolar surface, provides promising advantages for pulmonary drug delivery, moreover offering the chance to overcome the 'old problems' of classical administration routes, e.g. the first-pass effect and poor bioavailability after oral drug application. Besides these morphological aspects of the lung and aiming for a successful delivery concept, therapeutic aerosols must be generated and inhaled considering the principals of aerosol formation and deposition as is elucidated in the following section.

3.3. Aerosol Deposition within the Lung

Inside the respiratory system inhaled material deposits in different lung regions mainly depending on the aerodynamic particle diameter and the overall inhalation maneuver. Discrimination between the deposition sites is realized due to three different principal mechanisms: Brownian motion, sedimentation and impaction (Heyder, 1981). For particles smaller than 1 µm, Brownian motion will be the decisive mechanism for deposition in mainly alveolar regions of the lung. Particles sized 1–5 µm are suitable to enter and sediment within the tracheo-bronchial region, whereas particles larger than 5 µm will mainly be deposited in the oro-pharyngal airways due to impaction (Heyder et al., 1986; Oberdörster et al., 2005).

Interestingly, ultrafine particles of 0.005–0.2 µm are efficiently deposited in the deep lungs, whereas most of the particles sized 0.2–1.0 µm are exhaled again (Dolovich et

al., 2000; Heyder and Svartengren, 2002). A graphical impression of these important aerosol principles and the resulting particle deposition pattern is given in Figure 4.

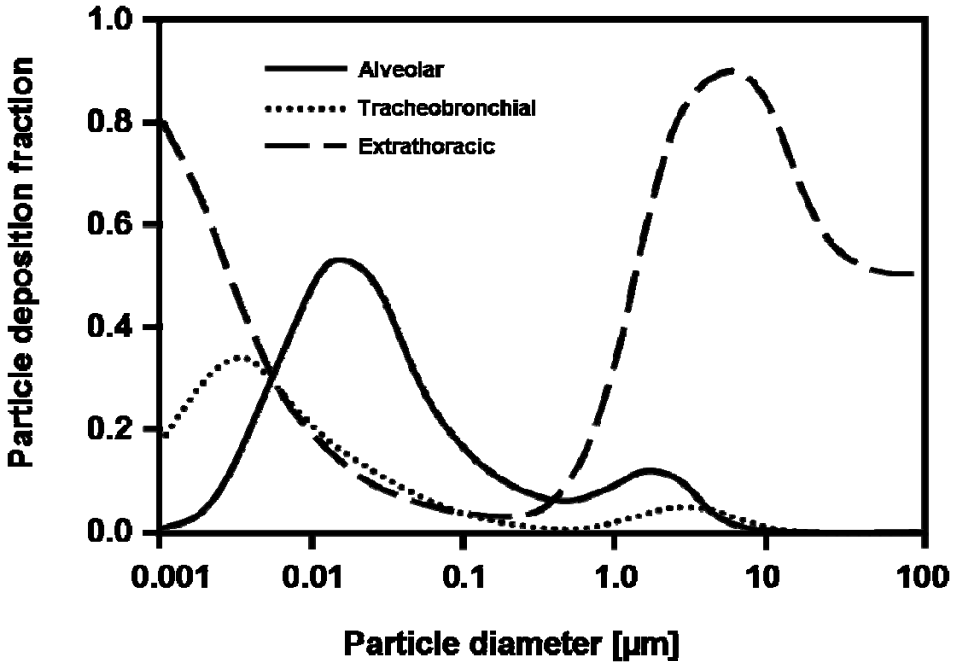

Figure 4: Regional Deposition of Particles within the Lung

Depending on particle size and the overall inhalation maneuver, the particles deposit within different regions of the lung. Although ultrafine particles of 0.005 – 0.2 µm are efficiently deposited in the deep lungs, this size range is currently not exploited for therapeutic aerosols. By courtesy of the Danish EPA (Report No. 12352008).

However, due to a lack of appropriate formulation technologies that can generate ultrafine drug particles (0.005–0.2 µm), and along with intrinsic limitations on the drug dose these particles can deliver within a reasonable aerosol volume or time of inhalation, this size range is not used for aerosol medicines at the moment.

It is obvious that incorrect pulmonary application inevitably results in a significantly reduced therapeutic drug effect. Nonetheless, most inhaled drugs are intended to reach the alveolar region, since the very thin epithelium (0.1–0.5 µm) and the huge alveolar surface (~140m^2) offer superior conditions for drug absorption. Overall the alveolar

surface accounts for more than 95% percent of the lungs total surface (Weibel, 1979). In this context, a defined and controlled inhalation maneuver is of utmost importance for regional targeting and normally intended alveolar deposition of the drug. The inspiratory flow rate and total volume act as decisive parameters for regional particle deposition (Bennett et al., 1999; Brand et al., 2000; Brown and Bennett, 2004). High flow rates (1000 ml/s) are correlated to an increased fraction of particles deposited within the central airways, whereas at slow flow rates (200 ml/s) the chance for alveolar deposition is increased (Scheuch et al., 2007). Accordingly, a major paradigm in aerosol drug delivery may be defined as "slow and steady wins the race" (Dhand, 2005).

So far the efficacy of many commercially available inhalation products still suffers from a big fraction of drug deposited in the airways (Hochrainer et al., 2005; Pitcairn et al., 2005). It is important to note that several more efficient technologies are available and hopefully will improve future inhalation therapy (Scheuch and Fischer, 2008; Scheuch and Siekmeier, 2007). However, the augmented use of such raising technologies is limited by the economic hurdles most new and cost intensive concepts are facing. In summary and with regard to pulmonary drug delivery devices, the work from the device or engineering side is mainly done, passing now the ball to the 'scientific team' to clarify what happens after the controlled deposition of the drug.

3.4. Lung Clearance Mechanisms

3.4.1. Airway Clearance

In parallel to the dissimilar morphological structure, there are also distinctive differences between clearance mechanism in the airways and the alveolar region. Deposition in the conducting airways normally occurs with particles or pathogens adhering to the sticky mucus layer lining the airway surface. Mucosal barriers in general can be found at various sites of the human body, lining the gastro intestinal

tract, intranasal epithelium, airways and more. In all cases the mucosal barrier serves as a shelter intended to protect the human body from exogenous influences such as bacteria, viruses or fungal spores. These pathogens normally interact with the viscous mucus layer, hence are immobilized and will be eliminated by clearance mechanisms present at the specific body sight.

Airway mucus is a viscous gel composed of highly glycosylated mucus proteins also called mucins (Desseyn et al., 2000; Thornton et al., 2008). After entrapment by the mucus layer, particles and pathogens are subsequently cleared from the deposition site as the mucus continuously moves proximally towards the upper end of the tracheal tube (Figure 5). Unidirectional mucus transport is realized due to energy transfer from beating cilia to the upper mucus layer. Airway cilia (~200 cilia per cell) are hair like cell appendages (5-7 µm) beating in a metachronal coordinated wave pattern, thereby transferring kinetic energy to the upper mucus layer during the forward stroke (Sleigh et al., 1988). Finally, entrapped material and mucus are swallowed and undergo further biochemical processing in the gastrointestinal tract.

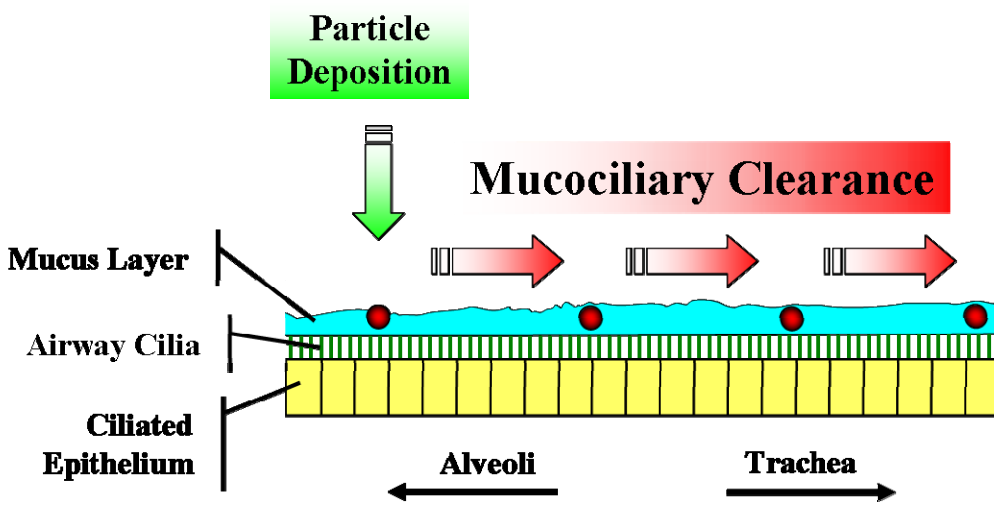

Figure 5: Mucociliary Clearance Scheme

After the particle deposited on the sticky airway mucus, both the mucus layer and the entrapped particle are cleared towards the upper end of the trachea. Continuous transport of the mucus layer is based on the metachronal beating of cilia.

In view of the average tracheal clearance velocity, as determined by noninvasive radiological techniques in healthy non-smokers, mucociliary clearance varied between 4.0 and 6.0 mm/min (Hofmann and Asgharian, 2003). Based on these results, the International Commission on Radiological Protection (ICRP) and the National Council on Radiological Protection (NCRP) adopted an average tracheal clearance velocity of 5.5 mm/min (ICRP, 1994; NCRP, 1997).

3.4.2. Alveolar Clearance

Drugs and particles that have been successfully deposited in the alveolar region will not be cleared by mucociliary clearance, since no ciliated cells are present in the deep lung. Here, alveolar macrophages (Figure 6) are the main important mechanism to defeat inhaled pathogens, particles and more (Moeller et al., 2005; Sibille and Reynolds, 1990).

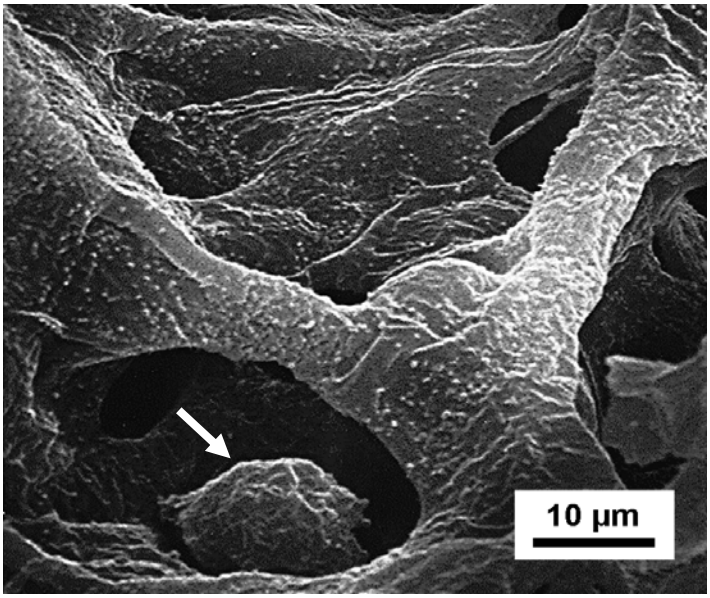

Figure 6: Top view of alveolar epithelium (SEM)

In the alveolar region, pathogens and inorganic particles are normally eliminated by alveolar macrophages, patrolling on the alveolar surface (see bottom left). By Courtesy of the Lawrence Berkeley National Laboratory.

Adult macrophages, derived from monocytes within the bone marrow, migrate towards the alveoli and patrol on the alveolar surface. With regard to the rate of particle elimination Geiser et al. were able to show that ultrafine TiO_2 particles, deposited in the lung of rats, are phagocytosed by the alveolar macrophages within hours (Geiser et al., 2005). Subsequently, alveolar macrophages either undergo mucociliary clearance upon ascending to the airways or actively migrate into the alveolar lymphatics for further involvement into immunomodulatory processes.

Comparing mucociliary airway clearance and alveolar clearance, the latter is unlikely to act as the limiting factor in inhalation therapy for several reasons:

- Many marketed products still suffer from poor drug delivery to the deep lung, consequently the active agent is mainly deposited in the airways.
- The alveolar surface accounts for about 95% of the lungs total surface, thus alveolar clearance, even if alveolar and airway clearance mechanisms would be comparable in efficiency, is unlikely to be as effective as mucociliary airway clearance.
- Considering the prevailing morphology in the airways versus the alveolar region, any drug or particle must overcome the thick and highly viscous airway mucus barrier, whereas the thin alveolar surface is designed for absorptive processes per se.

Consequently, mucociliary clearance (MC) essentially limits the benefit of many inhalation therapies: after initial inhalation and deposition, drug particles are rapidly cleared (4-6 mm/min!) and thus removed from the intended target site.

3.4.3. Mucociliary Clearance – State of the Art

Several *in vivo* as well as *in vitro* approaches have been realized in order to determine and investigate mucociliary transport rates (MTR) of drugs/particles in humans and animals. Due to anatomical as well as experimental reasons, direct *in vivo* measurements are complicated and presently available only for the human trachea (Foster et al., 1982; Leikauf et al., 1981; Mussatto et al., 1988; Toomes et al., 1981; Yeates et al., 1982).

The use of different experimental *in vivo* techniques produced a wide variability in the measured human MTR values, ranging from 3.6 to 21.5 mm/min. Reported tracheal MTR in rats and other animal species also display a wide range of values, presumably resulting from different experimental techniques as well (Hofmann and Asgharian, 2003). Hence, placing emphasis on the ethical aspects of such experiments, one might be in doubt about the scientific value of these results.

In order to overcome this unfavourable situation for *in vivo* studies, Rubin et al. developed the *in vitro* 'frog palate model' to investigate mucociliary clearance more detailed (Rubin et al., 1990). Leopard frogs (*Rana pipiens*) or bullfrogs (*Rana catesbiana*) are prepared by double pithing, i.e. bending the head forward and inserting a needle into the brain and the spinal cord. Subsequently, the jaw is disarticulated and the palate removed by cutting through from the junction of the posterior pharynx and oesophagus out to the skin of the back. The excised frog palate is focused under a dissecting microscope fitted with a micrometer scale, and the movement of mucus or entrapped particles is timed. At first instance, this model seemed to be a good approach to assess *in vitro* mucociliary clearance. Unfortunately, it turned out later that mucus transport on the frog palate was strongly influenced by season and other undetermined factors (Rubin et al., 1992). Besides this amphibian based concept, other researchers employed bovine or horse trachea explants to investigate *in vitro* mucociliary clearance (Gerber et al., 1997; Wills et al., 1995).

Though, both *in vitro* models require active treatment of the mucus which is likely to alter the native mucus properties and mucociliary transport rates in consequence.

Overall, *in vivo* studies on mucociliary clearance face many regulatory, ethical, and experimental problems; not least since it was shown that anaesthesia, which hardly can be avoided in these experiments, significantly influence mucociliary clearance rates (Ledowski et al., 2008; Ledowski et al., 2006). On the other hand, yet existing *in vitro* models often suffer from limited resources, time-consuming preparation, and critical preparation steps, such as chemical mucus depletion.

4. Aim of this Work

It is the extremely thin air-blood barrier (0.1 - 0.5 µm) and the huge surface area of the respiratory tract (~140m^2) which predominantly contribute to the lungs unique and promising barrier properties for pharmaceutical drug delivery. Nevertheless, mucociliary clearance still is a critical factor in pulmonary drug delivery, significantly limiting the therapeutic benefit of many inhalation therapies. Although the basic principles of mucociliary transport seem to be understood, there are many open questions on e.g. mucus-particle interaction and particle transport rates; not at least since the actual possibilities to investigate mucociliary clearance are rather limited and suboptimal. To overcome mucociliary clearance, a more detailed understanding of this clearance mechanism seems to be crucial and inevitable. In a next step, systematic studies utilizing different drug delivery approaches will be needed to identify most promising strategies. Consequently, the scientific demand for a new and more feasible *in vitro* method was obvious and the driving force behind the work presented here.

The major aims of this thesis were:

1) **To develop a new and feasible *in vitro* method, avoiding ethical as well as regulatory hurdles, to investigate mucociliary particle clearance.**

2) **To test the influence of critical parameters, such as temperature, humidity, and ciliotoxic drugs on mucociliary particle clearance.**

3) **To investigate clearance rates of different nanocarriers in order to identify parameters and promising strategies to overcome mucociliary drug/particle clearance.**

5. Development of the Embryonic Chicken Trachea (ECT) Based *In Vitro* Clearance Model

Parts of this chapter have previously been published in:

Henning A., Schneider M., Bur M., Blank F., Gehr P., Lehr C.-M. (2008): *Embryonic chicken trachea as a new in vitro model for the investigation of mucociliary particle clearance in the airways*. AAPS PharmSciTech, 9(2):521-527.

5.1. Abstract

Mucociliary clearance (MC) is an important defense mechanism of the respiratory system to eliminate inhaled and possibly noxious particles from the lung. Although the principal mechanism of MC seem to be relatively clear there are still open questions regarding mucociliary clearance of particles. Therefore, we have developed a new set-up based on embryonic chicken trachea (ECT) to investigate mucociliary particle clearance and related topics in more detail. ECT was placed in an incubation chamber after carbon particles were applied and tracked using optical microscopy. The aim of the study was to validate this new model by investigating the impact of temperature, humidity and drugs on mucociliary particle transport rates.

Particles were transported reproducibly along the trachea and clearance velocity (2.39 ± 0.25) mm/min was found to be in accordance to data reported in literature. Variation in temperature resulted in significantly reduced MC: (0.40 ± 0.12) mm/min (20°C); (0.42 ± 0.10) mm/min (45°C). Decreasing humidity (99% - 60%) had no significant effect on MC, whereas reduction to 20% humidity showed a significant influence on particle clearance. The use of different cilio- and mucoactive drugs, i.e. Propranolol, Terbutalin, and N-Acetylcysteine, resulted in altered MC according to the pharmacological effect of the substances: a concentration dependent decrease of MC was found for Propranolol.

From our results it is concluded that this new *in vitro* model can be employed to investigate mucociliary particle clearance in more detail. Hence, the model may help to understand and identify decisive physico-chemical parameters for MC and to answer open questions regarding the long-term clearance phenomenon, mucus-particle interactions, and more.

5.2. Introduction

The human lung as application site for active substances is of increasing importance for local (e.g. asthma, COPD) as well as systemic (e.g. Diabetes mellitus) therapy. The attractiveness of pulmonary drug delivery is attributed to the good absorption due to a huge alveolar surface area (70-140m²), unique barrier properties and avoidance of the first-pass effect (Corkery, 2000). Beside these therapeutic aspects there is a constant input of exogenous material into the lung triggered by breathing. Here, mucociliary clearance (MC) is a most important mechanism to eliminate inhaled and possibly noxious particles, bacteria and toxins from the central airways.

In the field of inhalation toxicology the aerodynamic diameter is termed to be a main decisive parameter. Particle classification is based upon a precise nomenclature which is inevitable for avoiding misunderstanding and confusion. Thus, ultrafine particles (UFP) are defined to be smaller than 100 nm in diameter, whereas particulate matter (PM) can be divided into inhalable PM_{10} ($d < 25$ µm) and respirable $PM_{2.5}$ ($d < 3.5$ µm). Depending on the aerodynamic diameter and the inhalation maneuver, particles will deposit in different regions within the respiratory system (Scheuch et al., 2007). Discrimination between deposition site of the particles is realized due to three different principal mechanisms: *impaction, sedimentation* and *Brownian motion* (Heyder, 1981). Particles sized > 5 µm will mainly be deposited in the oro-pharyngal region due to impaction, whereas particles sized 1-5 µm are suitable to enter the tracheo-bronchial region. When particle size is reduced to ≤ 1 µm, Brownian motion will be the decisive mechanism for deposition in mainly peripheral regions of the lung (Oberdörster et al., 2005).

To date exclusive deposition in either the bronchial or the alveolar region is not feasible and only can be optimized using special inhalation techniques, e.g. the shallow bolus technique for targeting the airways (Brand et al., 1995; Scheuch et al., 1989). Depending on the site of particle deposition, clearance is realized by different mechanisms: a) Mucociliary clearance (MC): the airways are covered by a mucus

layer that is transported by ciliary beating resulting in a fast removal of deposited particles. b) Alveolar macrophages: in the lung periphery no ciliated cells are present and alveolar macrophages are the defense mechanism in this region (Möller et al., 2004). As the present work describes the set-up of an *in vitro* test system to investigate mucociliary clearance, a closer look at the detailed morphological architecture, conditions and prerequisites in this area is appreciated.

In healthy individuals the mucus layer consists of the upper gel layer and the lower periciliary layer. The periciliary layer is a low viscosity fluid with a thickness of 5-7 µm which is slightly less than an extended cilium (Marttin et al., 1998). The mucus layer on top is a gel composed of a 3-dimensional polymer network of mucus glycoproteins or mucins. These mucin macromolecules are 70-80% carbohydrate, 20% protein and 1-2% sulphate bound to oligosaccharide side chains (Fuloria and Rubin, 2000; Matsui et al., 1998). About 3% of the mucus layer consist of mucins, while 90-95% consist of water, with electrolytes, serum proteins, immunoglobulins and lipids (Lethem, 1993; Verdugo, 1990).

Although optimum concentration for all components seems likely to exist, MUC5-AC and MUC5-B have been identified to be predominantly responsible for gel-forming and adhesive properties of airway mucus (Gray et al., 2001; Lillehoj and Kim, 2002). Alterations in secretion rate and MUC5-AC to MUC5-B ratio correlated with impaired mucociliary clearance can be found in several pathophysiological conditions of the respiratory system e.g. asthma, cystic fibrosis and COPD (Groneberg et al., 2002a; Groneberg et al., 2002b; Kirkham et al., 2002).

With regard to the human airway epithelium, 30-65% of the total airway epithelium are covered with ciliated cells, whereat each cell houses about 200 cilia (Blake and Sleigh, 1974). Cilia are motile hair-like appendages extending 5-7 µm from the surface of epithelial cells. They contain a central axoneme i.e. a bundle of microtubules arranged as nine outer doublets and one central pair (9*2+2 arrangement) (Satir and Christensen, 2007). Movement of the cilium is generated by

sliding movements of the microtubules under ATP depletion (Afzelius, 2000). Cilia beat in close coordination and adjust their frequency and phase of beating in response to neighboring cilia (Sleigh et al., 1988). Throughout the ciliary beat cycle, consisting of forward and backward stroke, cilia transfer kinetic energy to the on top located mucus layer predominantly during the forward stroke. Metachronal coordination and beat mechanics result in transport of the mucus layer towards the oesopharyngal region, where finally the mucus and entrapped material is swallowed.

Former studies could show that mucociliary clearance removes all particles larger than 6 µm in diameter within 24 hours from the human airways *in vivo*. For particles smaller than 6 µm a certain fraction was retained for more than 24 hours. Further reduction in particle size correlated with an increasing fraction of long-term cleared particles (Scheuch and Stahlhofen, 1987; Stahlhofen et al., 1986; Stahlhofen et al., 1990). Despite the phenomenon of long-term cleared particles, the effects of inhaled ultrafine particles and particulate matter on human health have been for years and still are under debate (Kreyling et al., 2006). However, the number of epidemiological studies indicating a correlation between exposure to particulate matter and adverse health effects increases constantly (Annesi-Maesano et al., 2007; Dominici et al., 2006).

By today the decisive parameters and mechanisms of particle long-term clearance are not understood and different hypotheses are under discussion: Depending on particle size and physico-chemistry a certain fraction of particles might penetrate into and through the mucus layer and thus escape from mucociliary clearance (Gehr et al., 1993; Gehr et al., 1996; Geiser et al., 2000; Peters et al., 2006; Schurch et al., 1990). In case that the mucus layer is not a fully closed blanket covering the surface of all airways, particles might penetrate directly into the periciliary layer after deposition and thereby undergo fast elimination (Iravani and As van, 1972; Matsui et al., 1998). Another reason for delayed clearance is possibly the deposition of a certain particle fraction in the peripheral lung although the airways are the primary target.

The aim of our study was to set up an *in vitro* model based on embryonic chicken trachea (ECT) to investigate mucociliary particle clearance under more complex constraints such as various **temperatures, humidities and drugs**. Histochemical characterization of the model was performed in order to check for functional development of ciliated cells, goblet cells, surfactant proteins, and differences compared to human tissue morphology.

Overall, this model will allow for exploring mucociliary clearance and mucus-particle interactions based on functional interaction of cilia and mucus. It is well suited for this approach since former experiments showed that embryonic chicken trachea is a valid substitute for human material in studying ciliary beat frequency and ciliary toxicity (Boek et al., 1999a, b; Merkus et al., 2001; Van De Donk et al., 1982).

5.3. Materials and Methods

5.3.1. Materials

Inorganic salts (E. Merck, Darmstadt, Germany); Activated carbon Ph.Eur. (E. Merck, Darmstadt, Germany); Fertilized chicken eggs (Lohmann Tierzucht GmbH, Cuxhaven, Germany); Octadecyltrichlorosilane (E. Merck, Darmstadt, Germany); Propranolol hydrochloride (Sigma-Aldrich Chemie GmbH, Steinheim, Germany); Terbutalin hemisulfate (Sigma-Aldrich Chemie GmbH, Steinheim, Germany); N-Acetylcysteine (Sigma-Aldrich Chemie GmbH, Steinheim, Germany); Uranyl acetate (Fluka AG, Zuerich, Switzerland); Lead citrate (Leica AG, Heerbrugg; Switzerland); Eppon resin (Fluka AG, Zuerich, Switzerland); Alcian Blue, 8GX standard (Sigma-Aldrich Chemie GmbH, Steinheim, Germany); Protein marker, SDS-Page standards, low range (BioRad, Muenchen, Germany); Anti-Surfactant Protein A, AB3420 (Millipore, Schwalbach Germany, formerly Chemicon); Goat anti-rabbit IgG, Alkaline Phosphatase conjugate, AP132A (Millipore, Schwalbach Germany, formerly Chemicon); NBT/BCIP Stock Solution (Roche Diagnostics Corporation, Indianapolis, USA). All chemicals used in the experiments were of highest available quality.

5.3.2. Breeding

Chicken eggs of SPF quality (specific pathogen free) were incubated in a breeding chamber (Hemel Breeding Instruments GmbH, Verl, Germany) at 37.8°C and 60% relative humidity for 19-20 days. During breeding, eggs were automatically turned 6 times per day, including a cooling period of 1 hour per day, to supply optimal conditions for development of the chicken embryo. Development of the chicken embryos was controlled by weighing as well as candling of the eggs (Figure 7A, 7B). Egg candling includes placing the egg on a plastic ring and subsequent illumination from below, using a regular 60W light bulb as light source. Thereby, a normal or

abnormal development status of the chicken embryo was ascertained by visual examination. Non-fertile eggs were displaced from the breeding chamber in order to minimize the risk of microbiological contamination of other eggs.

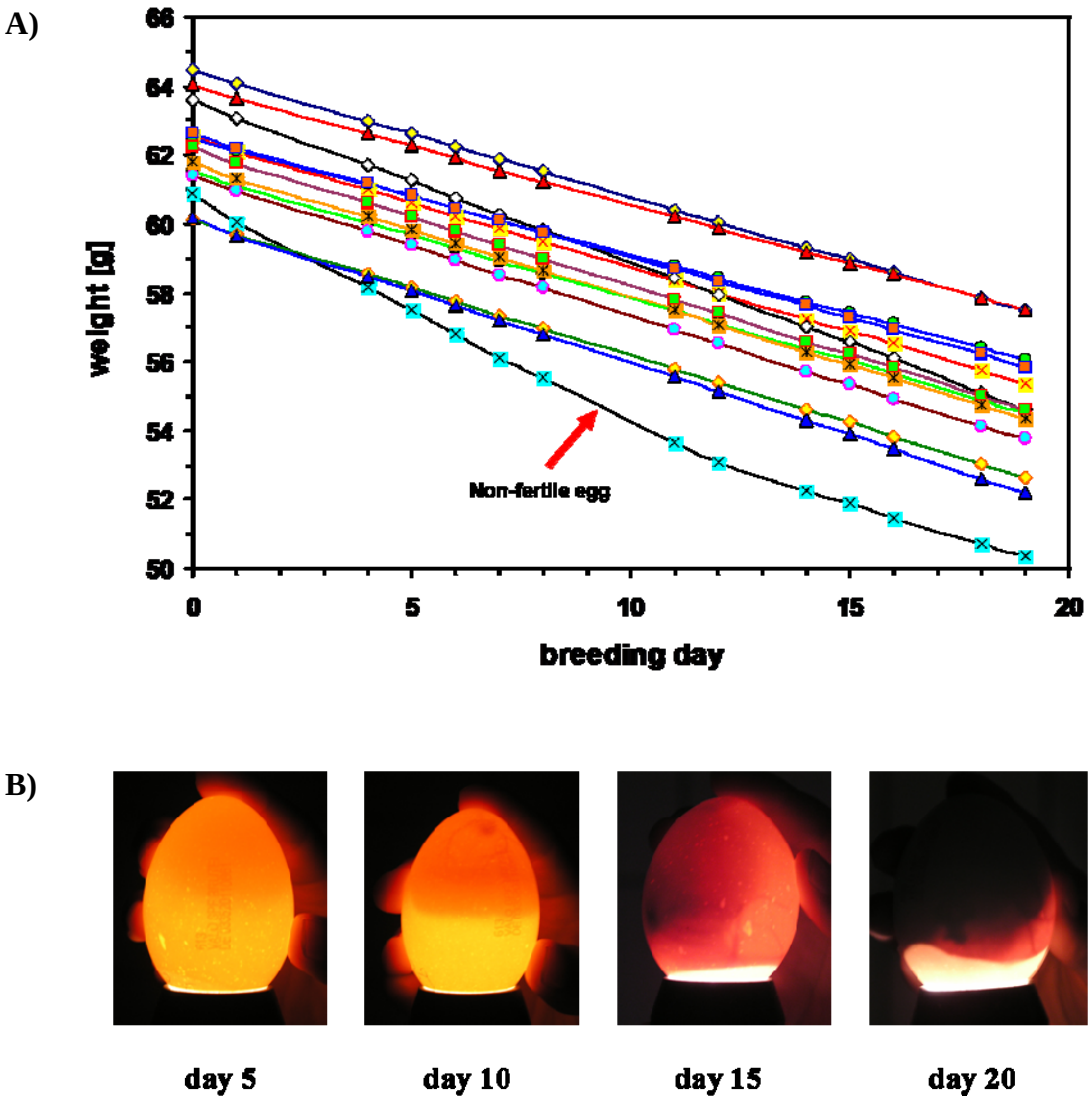

Figure 7: Breeding controls

A) The upper graph shows the results of egg weighing over the course of time. A non-fertile egg, indicated by the red arrow, shows an abnormal loss of weight during incubation in the breeding chamber. B) The picture series shows candling results at different stages of normal chicken embryo development. Normal or abnormal development status of a chicken embryo was ascertained by combined visual examination and weighing results.

5.3.3. Clearance Experiments

All clearance experiments were performed using freshly harvested embryo chicken trachea (Figure 8). After dissection the trachea was placed on gauze soaked with Locke-Ringer solution (LR). LR is an isotonic solution of NaCl 7.72g (132 mmol), KCl 0.42g (5.63 mmol), $CaCl_2$ x H2O (0.16g / 1.24 mmol), $NaHCO_3$ (0.15g / 1.79 mmol) and glucose anhydrous (1.00g / 5.55 mmol) in 1 litre of water. Prior to particle deposition the tracheal tube was cut oblong resulting in 2 tracheal half-pipes. Particle deposition on the half-pipes was realized utilizing a Dry Powder Insufflator™ Model DP-4 (PennCentury Inc., Philadelphia, USA) adopted from instillation experiments (Sakagami, 2006).

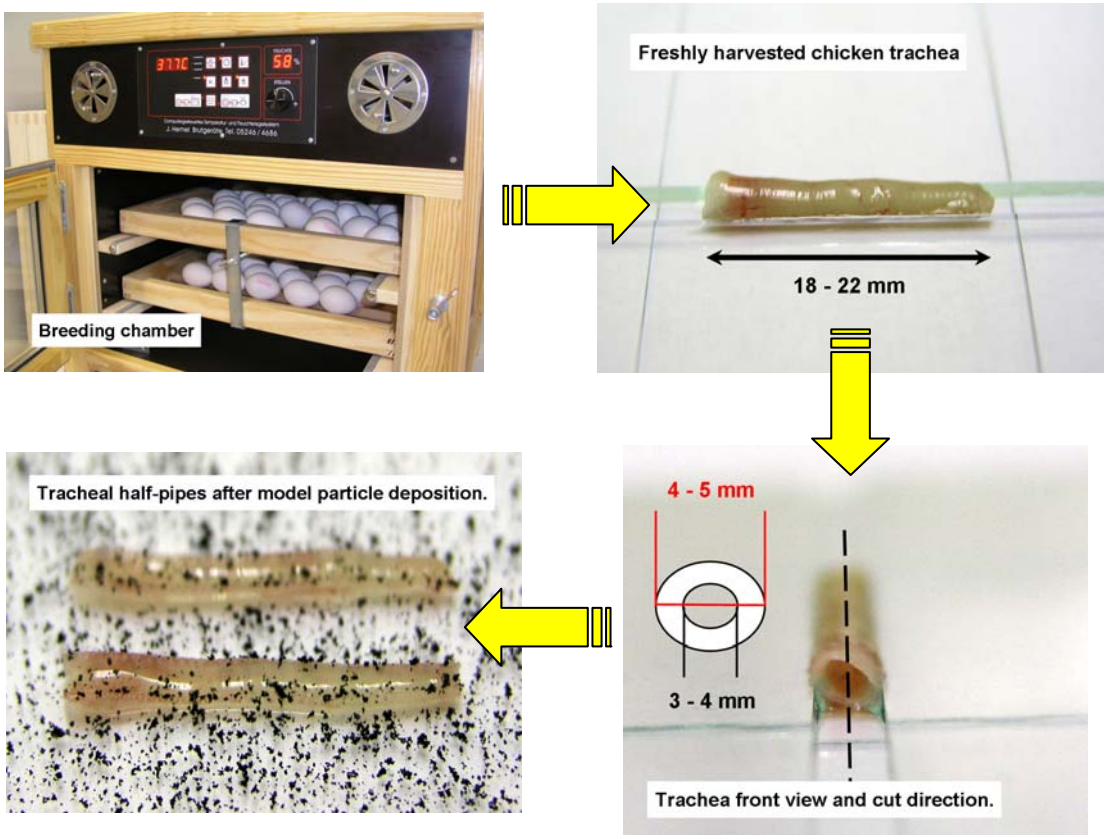

Figure 8: Breeding and Trachea Preparation

After breeding for 19-20 days (37.8°C; 60% rel. humidity) the embryonic chicken trachea was harvested and cut oblong. Subsequently, particles were deposited on the tracheal mucus and clearance was timed using appropriate imaging techniques.

Following particle deposition the tracheal tissue was transferred to a temperature and humidity controlled incubation chamber and subsequently placed under the microscope (Figure 9, Annex A.3).

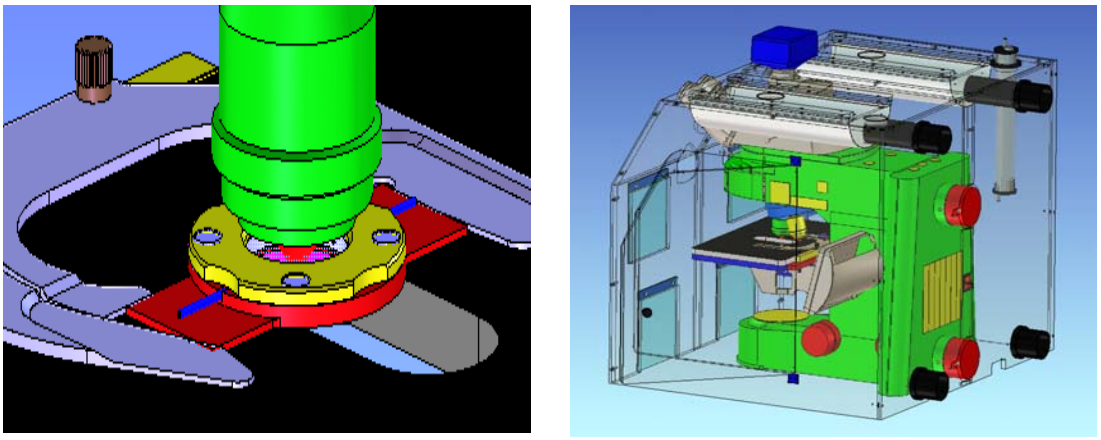

Figure 9: Experimental Set-up (see also Annex A.3)

Left: Incubation chamber placed under the microscope objective. The upper (yellow) part of the incubation chamber can easily be removed after turning the magnetic fixation by 45°. *Right:* In order to control the experimental temperature as well as humidity, the microscope was fully integrated within the isolation box.

To avoid critical fogging of the incubation chamber, the glass windows were modified using surface silanization methodology (Loebau et al., 1996; Metwalli et al., 2006). Briefly, the glass substrates were cleaned using a general glass cleaning protocol: immersion in NaOH (2.5 M) solution for 24 h, sonication in distilled water for 10 min, immersion in HCl (0.1 M) for 15 min, sonication in distilled water for 10 min and immersion in methanol for 5 min prior to the silanization step. Silanization of the glass substrates were performed by dip coating in 1% aqueous solutions of octadecyltrichlorosilane (OTS) for 15 min. Post-treatment steps include shaking in methanol for 5 min, rinsing in water for 10 min and finally spin drying (2000 rpm) for 5 min. The coated slides were baked at 110°C for 15 min and stored in a vacuum desiccator prior to use.

Carbon particles were applied as model particles to establish the experimental set-up due to easy visualization by transmission light microscopy. Particle size was 0.8–260 µm as determined by static light scattering (MasterSizer-2000, Malvern Inst., UK). Particle transport on the trachea was recorded for 10-20 seconds (AxioCam HSm, ZEISS, Germany) at various positions on the tracheal half-pipes using a LD Plan-Neofluar 10x/0.30 objective (ZEISS, Germany). Particle clearance velocity was calculated from 3-8 videos, and 3-6 single particles were calculated per video.

The effects of three drugs, i.e. *Propranolol, Terbutalin* and *N-Acetylcysteine*, already known to influence either ciliary beat frequency (CBF) or viscoelastic nature of the mucus layer, have been investigated. Tracheal tubes were incubated for 60 seconds in LR/drug solution or drug free LR solution (control) prior to particle deposition. A significant effect for Propranolol 1% (m/v) on CBF was already reported by Boek (Boek et al., 1999a). To investigate the model's sensitivity for a concentration dependent effect on mucociliary particle transport we tested Propranolol at 1% (3.4 mM), 0.1% (0.34 mM) and 0.01% (3.4 µM). Terbutalin and N-Acetylcysteine were both tested at 1% (m/v).

The influence of *temperature* (20-45°C) and *humidity* (20-99%) was investigated to test the model's robustness for various experimental conditions. Temperature and humidity in the incubation chamber were actively controlled and monitored online using a system provided by LIS (Life Imaging Services, Reinach, Switzerland). Results were examined for statistical differences by ANOVA using routine statistical software (SigmaStat 3.0).

5.3.4. Histochemical Characterization

Histochemical studies were realized in order to check for normal and functional development of ciliated cells, goblet cells, surfactant proteins (SP), and potential differences compared to human tissue morphology.

SEM/ TEM imaging:

For SEM imaging tracheal tissue was cut into slices of about 5 mm in width, dehydrated in ethanol, critical point dried and sputter-coated with gold. Samples were examined using a Philips XL 30-FEG scanning electron microscope (Philips AG, Zuerich, Switzerland) operating at 10 kV. For TEM imaging tissue was fixed for 24h in 0.03 M potassium phosphate buffer containing 2.5% glutar aldehyde. After fixation tissue was embedded in Eppon resin and cut to ultra-thin sections (60-80 nm) as described earlier (Gehr et al., 1978). The ultra-thin sections were transferred to uncoated 200-mesh copper grids and stained with uranyl acetate and lead citrate before examination.

Histology on formalin-fixed lung specimen:

Alcian blue, a group of polyvalent and basic dyes including copper in their molecule structure, was used to stain the tracheal sections. Strongly acidic sulfated or carboxylated mucosubstances (glycosaminoglycans) and mucins (glycoproteins) will be stained blue, nuclei will be stained pink to red, and cell cytoplasm will be stained pale pink. Tracheal tissue was fixed in 10% neutral-buffered formalin and embedded in paraffin at 58°C. Sections of 5 µm thickness were cut from the paraffin-embedded tissue and mounted on glass slides. Following on incubation in distilled water for 5 min the sections were transferred and stained with Alcian blue pH 2.5 (1% Alcian blue in 3% aq. Acetic acid) for 15 min. After thoroughly rinsing the sections in distilled water and counterstaining with neutral red for 1 min, rapid dehydration in absolute alcohol was used to fix the copper complex (Prophet et al., 1994). After a

final drying step the sections were examined microscopically to check for successful staining of the tissue compartments.

5.3.5. Surfactant Protein Analysis

Due to the relevance of surfactant proteins at the air-liquid interface, and presumably at the particle-mucus interface, the embryonic chicken trachea was analyzed for the presence of SP-A, the major protein in lung surfactant representing about 5–6% of its dry weight (Haagsman and Diemel, 2001). Freshly isolated embryonic chicken tracheas were rinsed with distilled water (3 x 5ml) in order to isolate the surfactant layer including the surfactant proteins from the inner tracheal surface. As positive control, fresh porcine tracheas from the local abattoir were processed in the same manner. Protein concentrations in the resulting solutions were determined using the BCA-Protein assay (Smith et al., 1985). Protein electrophoresis (15µg) was performed by SDS-PAGE (12% gels/ 180 min/ 80V) according to the method described by Laemmli (Laemmli, 1970). Western blotting (90 min/ 300mA) and subsequent immunostaining (Anti-SP-A: 1:5000) was employed for specific detection of SP-A in the embryonic chicken as well as porcine trachea lavage (Amin et al., 2001).

5.4. Results

5.4.1. Proof of Principle

Mucus and particles were clearly and reproducibly transported along the tracheal tissue. ***An exemplary video sequence on mucociliary particle transport is shown in the Annex (A.1).*** Clearance due to mucociliary interaction was successfully demonstrated by turning one of two tracheal half-pipes by 180°: particles were transported into different directions but always to the proximal end of the trachea (Figure 10).

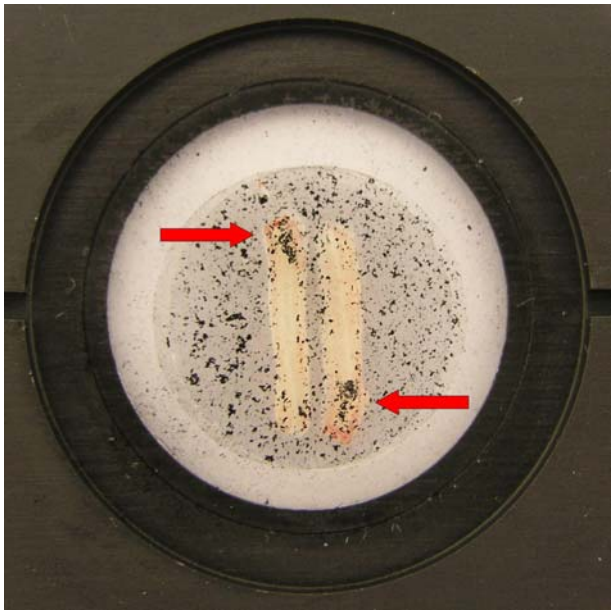

Figure 10: Proof of Principle

The picture shows the cleared inner half-pipes and the resulting accumulation of carbon particles at the proximal end of the trachea. In the clearance experiment (top view), carbon particles were transported into different but uniquely proximal direction after turning one of the tracheal half-pipes by 180°.

Furthermore, the tracheal mucus exhibited characteristic appearance, i.e. mucus streams and mucus flakes. Mucus transparency was according to the mucus grades (MG) classified by Gerber et al. (Gerber et al., 1997). Completely transparent mucus

(MG-1), transparent but slightly opaque mucus (MG-2), opaque mucus with slight surface relief (MG-3), and non-transparent, completely opaque mucus with marked surface relief (MG-4) were present on the tracheal epithelium.

5.4.2. Validation of the Experimental Set-up

As it was our intention to study the influence of temperature and humidity on mucociliary particle clearance, the overall experimental set-up was characterized with regard to its insulating properties. Temperature and relative humidity were measured in both the inlet and the outlet airflow of the incubation chamber (A.3B, page 76) and revealed no significant differences. After all instruments were switched on (t_0) the progression of temperature and humidification within the incubation chamber was determined (N = 3) after different predetermined time intervals (Figure 11, 12).

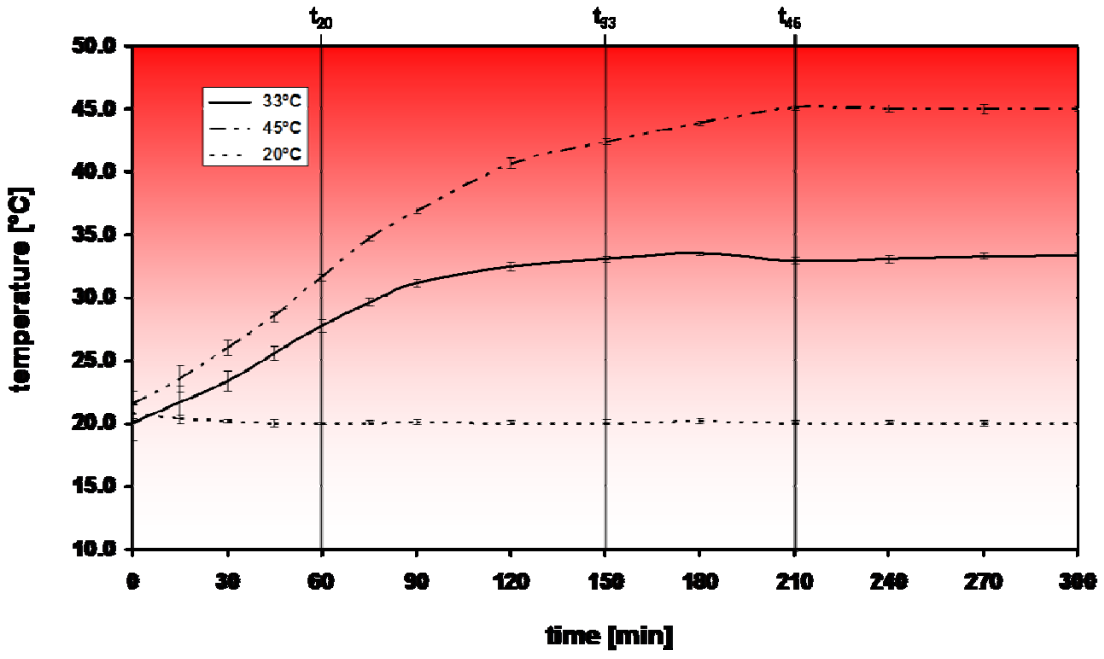

Figure 11: Experimental Set-up: Course of Temperature

From the graph it is obvious that equilibration time to ensure temperature stability must be adapted to the aimed and particular experimental temperature.

Comparing the course of humidity and temperature, the latter seems to be a more critical factor within our experimental set-up. A temperature of 20°C, 33°C, and 45°C was assured after 60 min, 90 min, and 210 min, respectively (Figure 11). In contrast, a relatively short equilibration time of about 60 min was suitable to provide 99% relative humidity for all different levels of temperature (Figure 12).

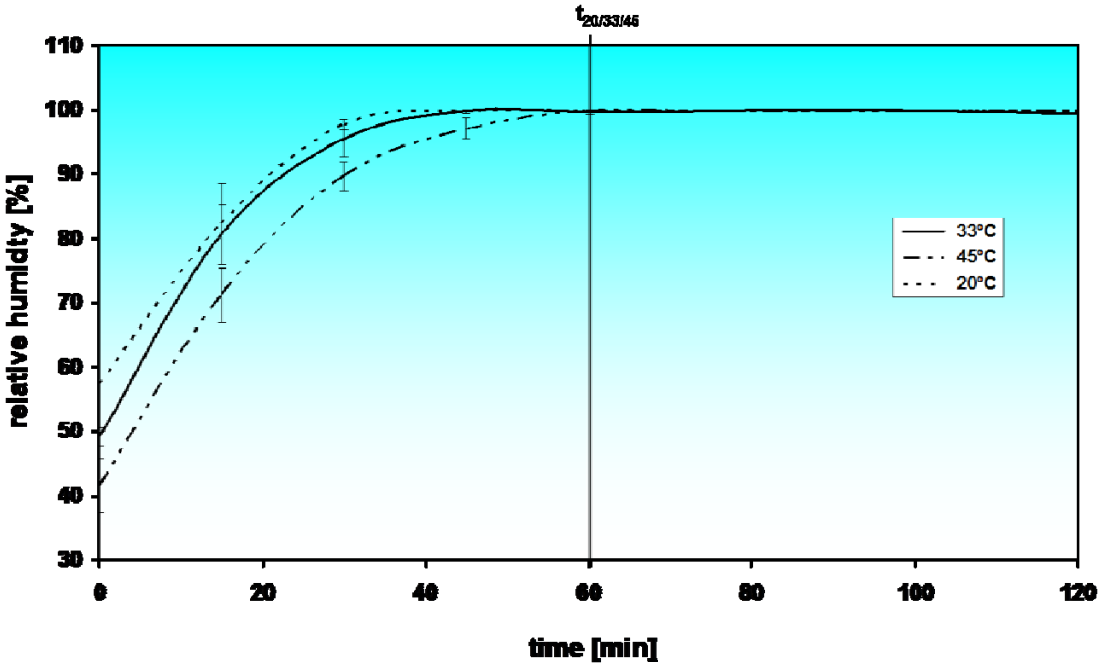

Figure 12: Experimental Set-up: Course of Humidity

Within the incubation chamber a relative humidity of 99% could be ensured after less than 60 min for all tested levels of temperature.

From the results of these validation experiments it is obvious that lead times to assure temperature and humidity equilibrium within the set-up must be adapted to the intended and aimed experimental temperature. Therefore, an equilibration period of 180 min was realized in all our experiments at 20°C and 33°C, and 210 min lead time for the studies at 45°C.

5.4.3. Temperature and Humidity

Decrease (20°C) as well as increase (45°C) in temperature resulted in significant reduction ($P \leq 0.001$) of mucociliary particle transport rates (MTR). MTR determined for 20°C, 33°C and 45°C was (0.40 ± 0.12) mm/min, (2.39 ± 0.25) mm/min and (0.42 ± 0.10) mm/min, respectively (Figure 13).

Variation of relative humidity between 60% and 99% had a non significant effect ($P \leq 0.001$) on particle transport. MTR was (2.29 ± 0.96) mm/min, (2.32 ± 0.70) mm/min and (2.39 ± 0.25) mm/min for 60%, 75%, and 99% relative humidity experiments, respectively. Further reduction to 20% relative humidity resulted in significantly decreased clearance rates (0.54 ± 0.37) mm/min ($P \leq 0.001$).

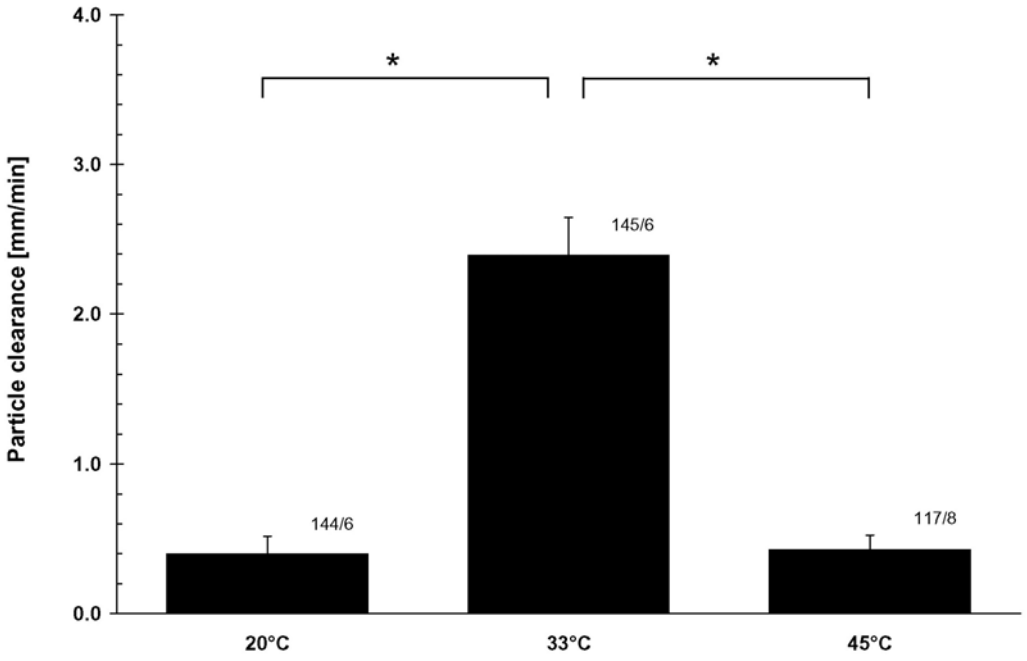

Figure 13: Influence of Temperature on MTR

Decreased (20°C) as well as increased (45°C) temperature resulted in significant reduction of particle transport rates (* $P \leq 0.001$). Numbers beside the bars e.g. "100/6" represent a total of 100 particles tracked on 6 tracheas.

5.4.4. Influence of Drugs

Particle clearance under influence of 3 drugs known to affect mucociliary clearance, namely Propranolol, Terbutalin, and N-Acetylcysteine was investigated (Figure 14). Propranolol (Pp) was capable of reducing or fully eliminating particle transport in a concentration dependent manner. No transport of particles could be observed after incubation in Pp-1% (3.4 mM) and Pp-0.1% (0.34 mM) LR/drug solution. Incubation in Pp-0.01% (0.034 mM) LR/drug solution resulted in significantly ($P \leq 0.001$) reduced transport (0.44 ± 0.21) mm/min compared to control experiments (C) (3.14 ± 0.41) mm/min, using only LR solution. Particle clearance under influence of Terbutalin (T) was significantly increased ($P \leq 0.001$) to (4.90 ± 0.62) mm/min, whereas N-Acetylcysteine (NAC) decreased particle transport significantly ($P \leq 0.001$) to (0.66± 0.20) mm/min.

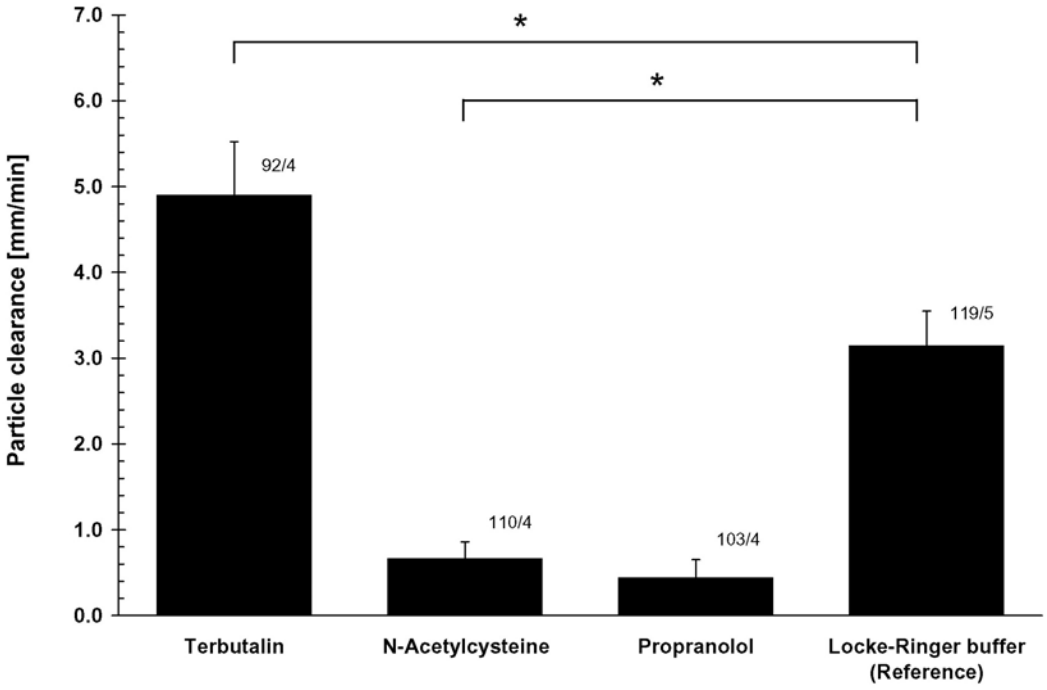

Figure 14: Influence of Drugs on MTR

Clearance velocity under the influence of drugs was significantly changed (* $P \leq 0.001$). Terbutalin (1%) increased, whereas N-Acetylcysteine (1%) and Propranolol (0.01%) reduced mucociliary particle clearance.

5.4.5. Histochemical Characterization

To assure presence of the morphological as well as histochemical factors required for functional mucociliary clearance, the epithelial topology of the embryonic chicken trachea as well as ultrastructure of the cilia was studied using Scanning Electron Microscopy (SEM) and Transmission Electron Microscopy (TEM).

TEM / SEM Imaging:

Cilia were found to be comparable to human respiratory cilia regarding cilia length (5-7 µm) and ultrastructure of the microtubules (Figure 15). The typical '9*2+2' arrangement of the inner (axoneme) and outer microtubules as well as the radial spokes can be clearly seen in the TEM studies. Morphology of the basal bodies, a basic parameter for functional and coordinated ciliary beating, exhibited normal topology and orientation. Microvilli were present in a characteristic manner at the epithelium surface.

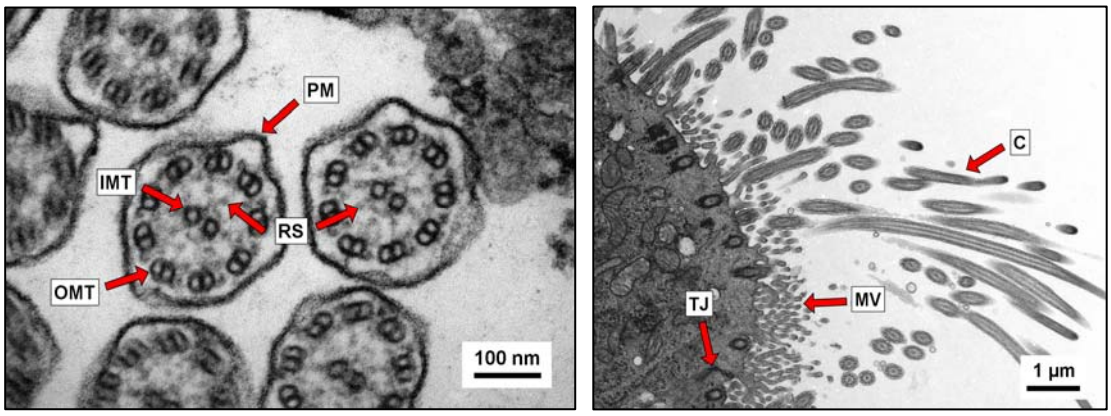

Figure 15: Cilia Morphology (TEM)

Left: Cross section of cilia; Outer Microtubules (OMT), Inner Microtubules (IMT), Radial Spokes (RS), Plasma Membrane (PM). *Right:* Cross section of embryonic chicken trachea epithelium; Tight Junctions (TJ), Microvilli (MV), Cilia (C).

Employing Scanning Electron Microscopy (SEM) to visualize and investigate the tracheal surface resulted in a surprising outcome: *Interestingly, airway macrophages are already present in the embryonic state of the chicken development,* as several SEM studies revealed airway macrophages adhering to the tracheal surface epithelium (Figure 16A).

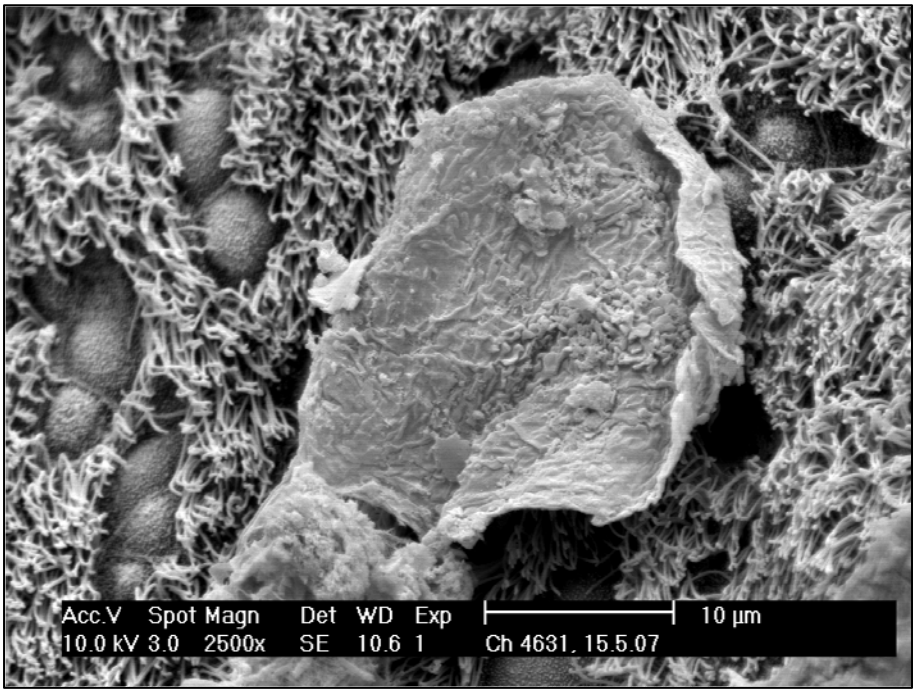

Figure 16A: Tracheal Surface (SEM)

The picture shows an airway macrophage patrolling on the tracheal surface of the embryonic chicken trachea. The tracheal epithelium exhibits typical airway morphology consisting of ciliated cells and non-ciliated goblet cells.

Furthermore, and in parallel to the previous TEM studies, SEM studies at different levels of magnification revealed a normal topology and distribution pattern of cilia, ciliated cells, and goblet cells (Figure 16B). The mucus layer, normally located on top of the ciliated airway epithelium, is not present in these studies as the trachea was several times rinsed with water in order to remove the mucus for imaging purposes.

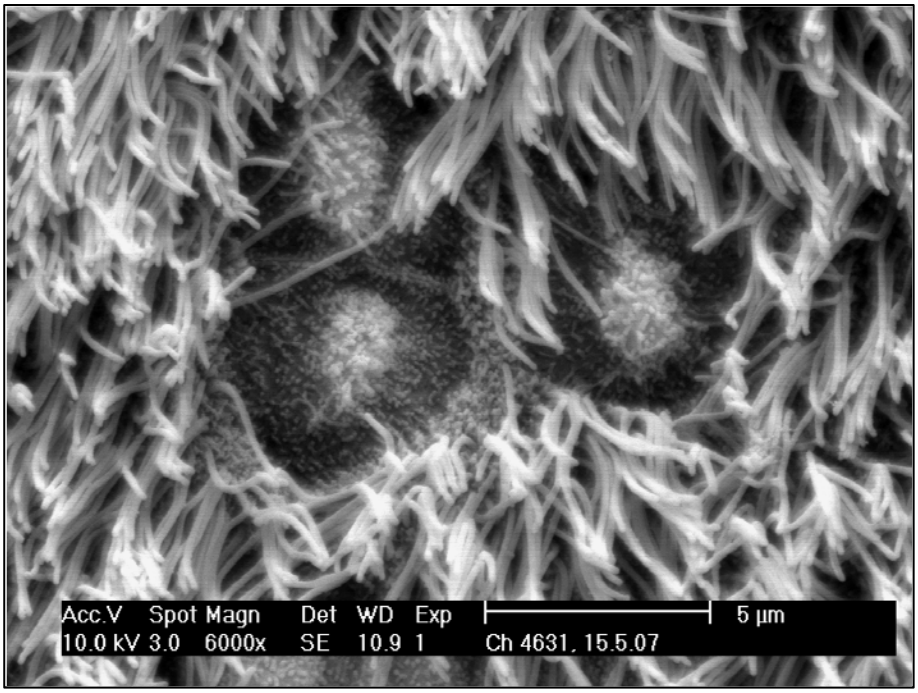

Figure 16B: Tracheal Surface (SEM)

Cilia on ciliated cells and non-ciliated, mucus producing goblet cells exhibit a characteristic topology and distribution pattern.

Paraffin sections:

Cross sections of the tracheal tissue showed normal morphology regarding cilia length and cilia density. Presence of goblet cells and of the airway mucus layer was successfully determined via characteristic Alcian blue staining (Figure 17, next page). Acidic mucins and mucosubstances present in the mucus layer, goblet cells, and hyaline cartilage are stained in deep blue. Cell cytoplasm and nuclei are typically stained in reddish and pink.

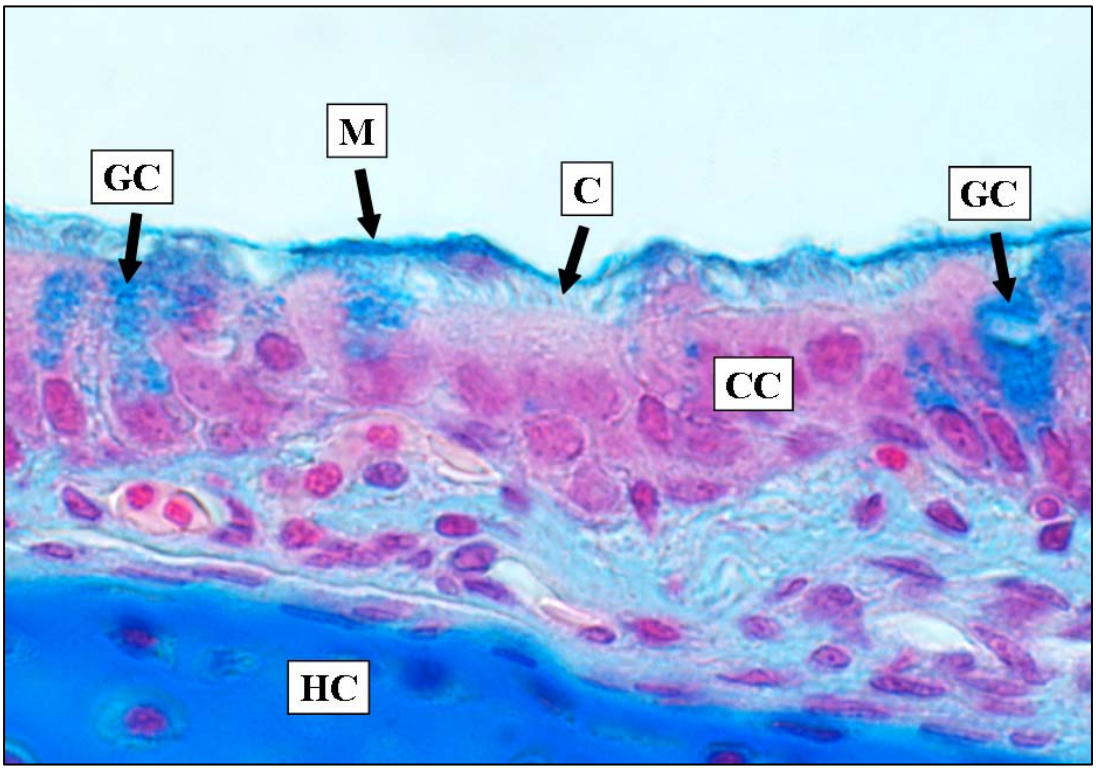

Figure 17: Alcian Blue Staining of Paraffin Embedded Tracheal Tissue.

The mucus layer (M), goblet cells (GC), and hyaline cartilage (HC) are present and exhibit characteristic staining. Cilia (C) on ciliated cells (CC). *x100 cross section*

5.4.6. Surfactant Protein Analysis

Lung surfactant is a complex mixture of lipids and proteins lining the inner surface of respiratory tract (Wright, 2004). Surfactant has two distinct functions. First, it reduces surface tension at the air-liquid interface of the lung - this function requires an appropriate mix of surfactant proteins and lipids. Second, surfactant also plays an important role in host defense against infection and inflammation. Due to the relevance of surfactant proteins at the air-liquid interface, the embryonic chicken trachea was analyzed for the presence of SP-A, the major protein in lung surfactant representing about 50% of the total surfactant protein mass (Hawgood, 1997). As can be seen from the experimental result, detection of SP-A in both embryonic chicken and porcine trachea lavage was positive (Figure 18).

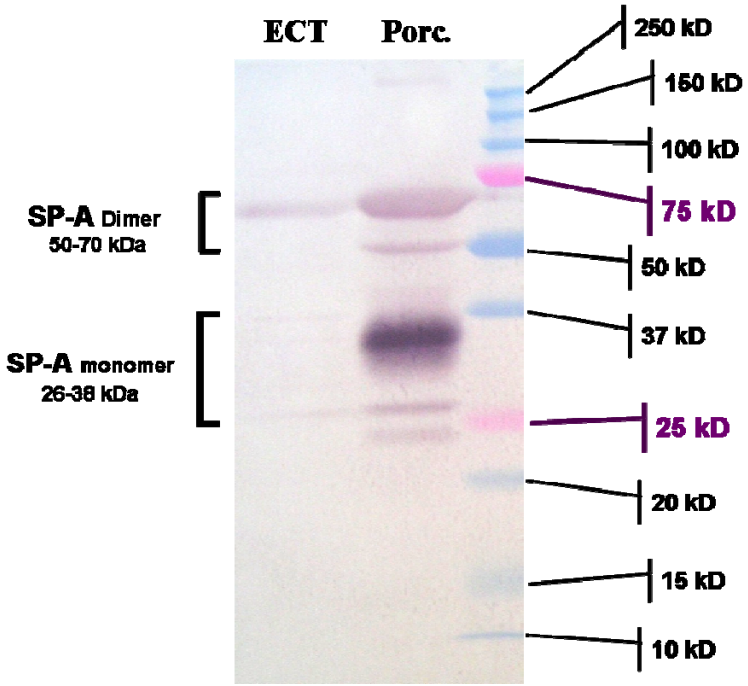

Figure 18: SP-A Immunoblot of Embryonic Chicken and Porcine Trachea Lavage.

For both the embryonic chicken (ECT) and the porcine (Porc.) trachea lavage a positive and characteristic immunoblot for SP-A could be observed.

Multiple bands in the range between 26-38 kDa and 50-70 kDa exhibit a characteristic distribution pattern and result from the multimeric SP-A structures and the multitude of post-translational SP-A modifications (Hermans and Bernard, 1999). A weaker signal for ECT in comparison to the porcine signal presumably results from a lower relative SP-A concentration in the ECT lavage, or a generally reduced antibody affinity for chicken SP-A multimers.

5.5. Discussion

Mucociliary clearance is a complex cleaning mechanism of the airways. Decisive parameters for mucociliary transport are ciliary beating, height of the periciliary layer (PCL) and viscoelastic properties of the mucus. Metachronal coordination of the beat pattern results in directional mucus transport only when transfer of kinetic energy from the cilia to the mucus layer is efficient. Thus, ciliary beat frequency (CBF) defines the maximum amount of kinetic energy to be transferred from the cilia to the upper mucus.

As known from literature CBF is correlated to temperature. Clairy-Meinesz reported that human cilia are almost immotile at 5°C. From 9°C to 20°C CBF increased constantly and values approximately doubled as the temperature increased by 10°C. Between 20°C and 45°C CBF was found to be constant at around 8-11 Hz. At 50°C cilia rapidly became immotile and cooling did not restore ciliary motility (Clary-Meinesz et al., 1992). Being aware of the CBF plateau between 20°C to 45°C and the comparability of human and chicken tissue at 33°C reported by Boek (Boek et al., 1999a), all control experiments were realized at 33°C and 99% relative humidity. Rheological properties of the mucus are important parameters regarding coupling efficiency and correlation of mucus transport rates and rheological properties have already been reported (Shah and Donovan, 2007a). If the elastic and the viscous modulus are out of range, kinetic energy will be lost and the mucus will not be propelled at normal velocity. The experimental results in our study demonstrate efficient interaction of mucus and beating cilia. Mucus exhibited characteristic transparency and structure (streams, flakes) and entrapped particles were reproducibly and unidirectionally transported along the tracheal tissue.

The results from the experiments at various temperatures clearly show a significant influence of temperature ($P \leq 0.001$) on mucociliary transport (Figure 13). Reduced clearance rates can be explained by a combinatory effect of reduced or less

coordinated CBF and changes in mucus rheology (King, 1979, 1980; Rubin, 1988). Clearance velocity (2.39 ± 0.25) mm/min for the control experiments (33°C / 99%) were found to be comparable to data reported in literature. Tracheal mucociliary clearance rates reported for rats, guinea pigs and rabbits are (1.9 ± 0.7) mm/min, (2.7 ± 1.4) mm/min and (3.2 ± 1.1) mm/min, respectively (Felicetti et al., 1981). The only reported value for human mucus velocity in the main bronchi is about 2.4 mm/min (Foster et al., 1980) which is in good accordance with our data. Decreasing relative humidity from 99% to 60% had no significant effect on transport rates and can be explained by a certain stability of MC function even under suboptimal environmental conditions. Thus, the duration of a single transport experiment (~10 min) might not be sufficient to change mucus properties, PCL height or CBF to a significant extent. Further reduction in relative humidity to 20% significantly influenced transport rates, suggesting that the model is sensitive for changes in humidity, moreover reflecting the *in vivo* situation where small changes should not affect MC dramatically.

The choice of different active substances was made with respect to their impact on the mucociliary transport rate, respectively the CBF. All drugs tested had a significant influence on mucociliary clearance (Figure 14). Terbutalin and Propranolol are both influencing CBF via β-receptor related signaling pathways. Terbutalin, acting as a β-adrenoceptor agonist, increases CBF by increasing intracellular levels of cyclic adenosine monophosphate (cAMP). On the contrary Propranolol, acting as β-blocker, reduces CBF via decrease of intracellular cAMP (Salathe, 2002). Mucociliary clearance for both drugs changes according to their respective pharmacological effect. For the experiments using Propranolol at various concentrations a concentration dependent effect could be determined, suggesting that the model exhibits sensitivity for drugs in a concentration dependent manner. The influence of N-Acetylcysteine (NAC) resulted in a significant reduction of mucociliary transport rates and can be explained by a significant change of mucus rheology. NAC is known to sever

disulfide bonds, thus diminishing crosslinking of the mucin network. In consequence, the viscosity as well as the elasticity of the mucus gel is reduced and the energy transfer from the cilia to the upper mucus layer is less efficient (Fuloria and Rubin, 2000).

Histochemical studies were performed to investigate functional development of ciliated cells, goblet cells, presence of surfactant proteins (SP-A), and possible differences compared to human tissue morphology. In the outcome, ECT morphology was found to be comparable to human tracheal tissue. Cilia length, cilia density and orientation of the basal bodies exhibit characteristic structure and orientation. Presence of goblet cells, mucus, and SP-A was successfully determined by Alcian blue staining and immuno-detection, respectively. Hence, all structures essentially required for mucociliary clearance and mucus particle interaction are present on the embryo chicken trachea.

Several model systems based on frog palate, horse or bovine trachea are already available (King, 1998). Compared to those *in vitro* models the ECT model is favorable for several reasons: 1) Breeding eggs are commonly available in SPF (specific pathogen free) quality which reduces the costs and risks for biological contamination of the experimentalist and instruments to a minimum. 2) Eggs are easy to handle, do not need to be fed, and can be stored for up to 1 week prior to fully automated breeding. 3) As a result from 1) and 2) a high standardization for the ECT model is possible. This argument gains even more importance considering the fact that embryonic chicken trachea is an already validated model for investigating ciliary beat frequency (Boek et al., 1999a, b).

These crucial aspects allow for generating a profound data basis. In experiments utilizing porcine or bovine tracheal tissue, such standardization may hardly be achieved as tissue from the local abattoir often undergoes critical but inevitable treatment e.g. cleaning with hot water steam, flames, and more. Transportation to the

laboratory takes valuable time and experimental results may include artifacts. Moreover, housing conditions for the animals are not standardized, thus bacterial contamination or lung pneumonia can not be excluded. Raising animals for experimental use under best possible standardized conditions would be an option but suffers from increasing costs and the controversial discussion on ethical as well as regulatory aspects.

5.6. Conclusion

The pulmonary route is considered as a promising target for drug and protein delivery. However, there are still open questions regarding long-term clearance of particles from the airways and mucus-particles interactions. Hitherto, ECT has been utilized and validated for CBF measurements under influence of various chemical substances. The aim of our study was to set up an *in vitro* model based on chicken trachea in order to investigate MC of particles under more complex constraints such as temperature, humidity and various drugs. Thus, MC in the experiments is a result of ciliary beating and effective energy transfer from cilia to the mucus.

From our results we conclude that embryo chicken trachea can be employed to investigate the influence of cilio- and mucus-active drugs or particles on MC. The model shows a stability reflecting the *in vivo* situation where small changes are not supposed to impact dramatically on MC. Nevertheless, the ECT model is sensitive to changes in environmental conditions regarding temperature and humidity. Furthermore, the model allows for investigating the impact of drugs as could be shown for substances already known to influence clearance rates. As well this holds for the tissue response of the ciliotoxic substance Propranolol, which shows a concentration dependent decrease of MC as a result of the reduced ciliary function, as for Terbutalin and its clearance enhancing effect. Changes in mucus structure and the correlated rheological properties as achieved with N-Acetylcysteine can be monitored as well.

Therefore, the ECT *in vitro* clearance model is a powerful tool to investigate particulate impact on the clearance functionality of the tracheal airway. Future experiments utilizing different sized and/or modified (nano) particles shall help to understand and identify decisive physico-chemical parameters for MC and to answer open questions on the particle long-term clearance phenomenon.

6. Influence of Particle Size and Surface Properties on Mucociliary Particle Clearance

Parts of this chapter will be submitted to the Journal of Controlled Release.

Henning A., Schneider M., Nafee N., Rytting E., Kissel T., Grafahrend D., Klee D., Lehr C.-M. (2009): *Influence of particle size and surface properties on mucociliary clearance from the airways*.

6.1. Abstract

Mucociliary clearance (MC), designed by evolution to eliminate inhaled and possibly noxious material from the airways, considerably limits the benefit of pulmonary drug delivery. Although the principal mechanism of MC seems to be understood, there are many open questions regarding physico-chemical factors determining the rate of mucociliary particle clearance. In this study a chicken trachea based *in vitro* model was used to investigate the effect of particle size and different particle surface properties on mucociliary particle clearance. The influence of particle size was investigated using polystyrene particles sized between 50 nm and 6000 nm. The effect of zeta-potential and mucoadhesive particle properties was tested using nanoparticles produced from different PLGA-copolymers, including chitosan-PLGA and PEG-PLGA branched polyesters as therapeutic relevant materials.

Experimental results showed no significant influence of polystyrene (PS) particle size on mucociliary transport rates (MTR): 50 nm, 100 nm, 1000 nm, and 6000 nm poly styrene particles were cleared at 3.2 ± 0.6 mm/min, 3.8 ± 0.8 mm/min, 3.8 ± 0.9 mm/min, and 2.9 ± 0.6 mm/min, respectively. In contrast, particle clearance of different PLGA-co-polymeric nanoparticles exhibited significant differences: Chitosan-PLGA particles were transported by a factor of 4-5 slower than blank PLGA spheres: 0.7 ± 0.3 mm/min versus 3.2 ± 0.6 mm/min. High molecular weight PEG_{10kDa}-PDLLA nanoparticles were transported at 2.8 ± 0.4 mm/min, whereas low molecular weight PEG_{5kDa}-PLGA particles were transported significantly faster at 5.9 ± 1.7 mm/min.

Overall, particle size and zeta-potential seem to be relatively uncritical, whereas mucoadhesive interactions, determined by the particles' chemical structure, can significantly impact on mucociliary particle clearance. Considering these findings in future drug formulation might help to control or even overcome mucociliary clearance and thereby optimize the benefit of inhalation therapy.

6.2. Introduction

Mucosal barriers can be found at various sites of the human body, covering the gastrointestinal tract, female reproductive tract, intranasal epithelium, airways, and more. These mucosal barriers protect the human body from invading pathogens such as viruses, bacteria, and fungal spores. Pathogens as well as other insoluble particles normally adhere to the viscous mucus layer, where they are immobilized and will be eliminated by clearance mechanisms present at the specific site.

Inside the respiratory system, inhaled material deposits in different lung regions depending on the aerodynamic particle diameter and the overall inhalation maneuver (Scheuch et al., 2007). Discrimination between the deposition sites is realized due to three different principle mechanisms: *Brownian motion, sedimentation* and *impaction* (Heyder, 1981). For particles sized smaller than 1 micron, Brownian motion will be the decisive mechanism for deposition, mainly in the alveolar regions of the lung. Particles sized 1–5 microns are suitable to enter and sediment within the tracheobronchial region, whereas particles larger than 5 microns will mainly be deposited in the oropharyngeal airways due to impaction (Oberdörster et al., 2005). Both the oropharyngeal and the tracheobronchial regions are part of the central lung and airways. Since there are different clearance mechanisms in the alveolar lung region, this must be considered if mucociliary particle clearance is the subject of investigation, as is here.

Upon deposition in the airways, particles normally are trapped by the sticky mucus layer, lining the airway surface. Airway mucus is a gel composed of a 3-dimensional network of mucus glycoproteins (mucins). The mucin macromolecules consist of 70 – 80% carbohydrate, 20% protein and 1 – 2% sulphate bound to oligosaccharide side chains (Fuloria and Rubin, 2000; Matsui et al., 1998). About 3% of the mucus layer consists of mucins, while 90–95% consists of water with electrolytes, serum proteins, immunoglobulins and lipids (Lethem, 1993; Verdugo, 1990). After entrapment by the mucus, particles are subsequently cleared from the deposition site

as the viscous mucus layer continuously moves proximally towards the upper end of the trachea. Unidirectional transport is realized due to controlled energy transfer from beating cilia to the upper mucus layer. Airway cilia (~200 cilia per cell) are hair like cell appendages (5-7 μm) beating in a metachronal coordinated wave pattern, thereby transferring kinetic energy to the upper mucus layer during the forward stroke (Sleigh et al., 1988). Finally, particles and mucus are swallowed and undergo further biochemical processing in the gastrointestinal tract.

With respect to drug delivery, the lung's unique barrier properties and large surface area (~140 m²) offer some promising advantages over other routes, e.g. oral drug delivery, which is often associated with poor drug permeability and the first-pass effect. Furthermore, there has been a sharp increase over the last 40 years in the global prevalence, morbidity, and mortality associated with asthma and COPD (Chronic Obstructive Pulmonary Disease), particularly in children. Approximately 300 million people worldwide currently have asthma, and its prevalence increases by 50% every decade. According to new estimates for 2030, COPD is predicted to become the third leading cause of death (WHO, 2008). As a consequence, more and more medical and also economical attention will be given to asthma and COPD therapy (Bousquet et al., 2007). Therapeutic intervention for both diseases requires repeated daily drug application, depending on the actual status and severity of the disease. Here, mucociliary clearance (MC), originally designed to clear pathogens and other exogenous material from the airways, essentially limits the benefit of inhalation therapy: after the initial inhalation and deposition, drug particles are rapidly cleared and thus removed from the intended target site.

Throughout the last decade, many different approaches have been realized in order to improve pulmonary drug delivery. Nevertheless, inhalation therapy still is problematic and related to many open questions on mucociliary particle clearance and mucus-particle interaction. Former studies could show that MC removes all particles larger than 6 μm in diameter within 24 hours from the human airways, whereas for particles smaller than 6 μm a certain fraction was retained for more than 24 hours.

Interestingly, further reduction in particle size (<<6 µm) was correlated to an increasing fraction of long-term retained (> 24 h) particles (Möller et al., 2004; Scheuch and Stahlhofen, 1987; Stahlhofen et al., 1986; Stahlhofen et al., 1990). If this clearance phenomenon is correlated to particle size, the particle's inherent physico-chemical properties, or if other factors determine mucociliary particle clearance still has to be answered.

Thus, the aim of our study was first to investigate the **influence of particle size**, and secondly to test the **effects of different particle surface properties**, determined by the chemical surface structure, on mucociliary particle clearance. Experiments were realized under standardized conditions using the previously established ECT *in vitro* model. The influence of particle size was investigated employing hydrophobic polystyrene (PS) model particles in a size range between 50 nm and 6000 nm. The effect of zeta-potential and particle surface properties was tested using various nanoparticles produced from different polymers (Table 1, Annex A.2), namely PLGA (I), chitosan-PLGA (II), PVA-g-PLGA (III), DEAPA-PVA-g-PLGA (IV), P(VS-VA)-g-PLGA (V), PEG-PDLLA (VI), and PEG-PLGA (VII).

Table 1: Polymers used for Particle Preparation and Abbreviations used in the Text.

Abbreviation	Polymer	Polymer No.
PLGA	poly(D,L-lactide-co-glycolide)	I
chitosan-PLGA	chitosan-poly(D,L-lactide-co-glycolide)	II
PVA-g-PLGA	poly(vinylalcohol)-graft-poly(D,L-lactide-co-glycolide)	III
DEAPA-PVA-g-PLGA	diethylaminopropylamine-poly(vinyl-alcohol)-graft-poly(D,L-lactide-co-glycolide)	IV
P(VS-VA)-g-PLGA	poly(vinylsulfonate-covinyl alcohol)-graft-poly(D,L-lactide-co-glycolide)	V
PEG-PDLLA	poly(ethyleneglycol)-block-poly(D,L-lactide)	VI
PEG-PLGA	poly(ethyleneglycol)-block-poly(D,L-lactide-co-glycolide)	VII

PLGA (I) and chitosan-PLGA (II) were included to test the influence of a multi-functional polymer which has been used for biomedical as well as drug delivery applications before (Agnihotri et al., 2004; Lehr, 2000; Rabea et al., 2003). Polymers III/IV/V (Rytting et al., 2008; Wang et al., 2008) were kindly provided by Prof. Dr. Thomas Kissel (Philipps Universität Marburg, Marburg, Germany). Polymers VI/VII (Grafahrend et al., 2008; Neuss et al., 2008) were kindly provided by Prof. Dr. Doris Klee (Chair of Textile Chemistry and Macromolecular Chemistry of RWTH Aachen, Aachen, Germany).

Overall, identification of critical parameters for mucociliary particle clearance and mucus-particle interaction shall be employed to optimize the development of inhalable drug formulations. This in consequence may help to improve pulmonary drug delivery and to develop new therapeutic strategies for a continuously increasing number of patients suffering from asthma, COPD and other chronic respiratory diseases.

6.3. Materials and Methods

6.3.1. Materials

Inorganic salts (E. Merck, Darmstadt, Germany), fertilized chicken eggs (Lohmann Tierzucht GmbH, Cuxhaven, Germany), various sized (50nm/100nm/ 1000nm/6000nm) polystyrene particles (Fluoresbrite®, Polysciences, Eppelheim, Germany), poly-D,L-lactide-co-glycolide (70:30) (Polysciences Europe GmbH, Eppelheim, Germany), polyvinyl alcohol; Mowiol® 4-88 (Kuraray Specialities Europe GmbH, Frankfurt, Germany), ultrapure Chitosan chloride: Protasan® UP CL113 with a molecular weight of <150 kDa (FMC BioPolymer AS, Oslo, Norway), ethyl acetate (Fluka Chemie GmbH, Buchs, Switzerland), poly(vinylalcohol)-graft-poly(D,L-lactide-co-glycolide), diethyl-aminopropylamine-poly(vinylalcohol)-graft-poly(D,L-lactide-co-glycolide), and poly- (vinylsulfonate-covinyl alcohol)-graft-poly(D,L-lactide-co-glycolide), in the following termed polymers III/IV/V (Rytting et al., 2008; Wang et al., 2008); poly(ethyleneglycol)-block-poly(D,L-lactide) and poly(ethyleneglycol)-block-poly(D,L-lactide-co-glycolide), in the following termed polymers VI/VII (Grafahrend et al., 2008; Neuss et al., 2008). All chemicals used were of the highest available quality.

6.3.2. Particles

A) Polystyrene particles:

Commercially available fluorescent polystyrene particles were used to investigate the influence of particle size and correlated factors on mucociliary particle clearance. Particles employed for experiments were sized 50nm, 100nm, 1000nm, and 6000nm, exhibiting all the same chemical polymer structure.

B) Polymeric nanoparticles produced from different polymers:

In order to investigate the effects of zeta-potential, mucoadhesion, and chemical polymer structure on mucociliary particle clearance, various polymers, namely PLGA (I), chitosan-PLGA (II), PVA-g-PLGA (III), DEAPA-PVA-g-PLGA (IV), P(VS-VA)-g-PLGA (V), PEG-PDLLA (VI), and PEG-PLGA (VII), were used to generate polymeric nanoparticles (Table 1).

Particle preparation was according to established protocols using the solvent-diffusion-evaporation (polymers I/II) or the solvent-displacement technique (polymers III-VII) (Ganachaud and Katz, 2005; Nafee et al., 2007; Ravi Kumar et al., 2004). To allow for fluorescence imaging of the particles, polymers were labeled by covalent binding of fluorescein amine or 7-MCCA (7-methoxy-coumarin-3-carbonylazide) following previously described protocols (Horisawa et al., 2002; Weiss et al., 2006). Size and zeta-potential of all particles were determined via Photon Correlation Spectroscopy and Laser-Doppler Anemometrie using a Zetasizer Nano ZS (Malvern Inst., Malvern, UK). Due to rapid sedimentation, 6000 nm polystyrene particles were not accessible for characterization using the Zetasizer Nano ZS. Here, particle size was determined using a MasterSizer 2000 (Malvern Inst., Malvern, UK), but these particles' zeta potential could not be determined.

6.3.3. Mucociliary Clearance Experiments

Clearance experiments including trachea preparation and particle tracking were performed as described previously. Briefly, chicken eggs of SPF quality (specific pathogen free) were incubated in a breeding chamber (Hemel Breeding Instruments GmbH, Verl, Germany) at 37.8°C and 60% relative humidity. Embryonic chicken tracheas were harvested on day 19–20 and clearance experiments (20 min) were performed directly after dissection. Particle deposition on the trachea surface was realized using a Microsprayer™ (PennCentury Inc., Philadelphia, USA), originally

developed for *in vivo* instillation experiments. Prior to particle deposition the tracheal tube was cut oblong resulting in two tracheal half-pipes. Particles were nebulized from aqueous suspension (50 µl) at constant mass concentrations (0.2 mg/ml) using a set-up previously established by Blank et al. (Blank et al., 2006). After particle deposition, the tracheal tissue was transferred to a temperature (33°C) and humidity (99%) controlled incubation chamber and subsequently placed under the microscope (AxioImager-M3, ZEISS, Germany).

Mucociliary clearance of the particles was visualized via fluorescence microscopy (LD Plan-Neofluar 10x/0.30 20x/0.40, ZEISS, Germany) and recorded for 10–20 seconds (AxioCam HSm, ZEISS, Germany) at various positions on the tracheal half-pipes. Mucociliary transport rates (MTR) were calculated from 5-7 clearance experiments, considering 3-8 tracking videos and 3-8 particles tracked per video, respectively. All experimental results were examined for statistical differences (One Way-ANOVA, t-test) using routine statistical software (SigmaStat 3.0).

6.4. Results

6.4.1. Influence of Particle Size

Size of the polystyrene particles (PS) as measured by Photon Correlation Spectroscopy was in good agreement with diameters indicated by the manufacturer label. Zeta-potentials were found to be highly negative and comparable for all different sized polystyrene particles, as was expected due to the identical polymer composition. By stepwise increasing particle size from 50 nm to 6000 nm, the size correlated factors, such as particle surface and particle number, considerably decreased and hence varied between the polystyrene experiments. To consider this, relations of the particles diameter [d], surface [A], and number [N] were calculated from the results of polystyrene particle characterization (Table 2).

Table 2: Results of Polystyrene (PS) Particle Characterization

Size of the particles was in good agreement with diameters indicated by the manufacturer label. Particle diameter (d), polydispersity index (PDI), zeta-potential (Zeta), factors for particle diameter (f_d), total surface (f_A), and particle number (f_N) in comparison to 6000 nm PS particles.

Particles	Diameter [nm]	PDI [-]	Zeta [mV]	f_d [-]	f_A [-]	f_N [-]
PS 6.0	6074	*	*	1	1	1
PS 1.0	965	0.077	-62	6.29×10^0	3.96×10^1	2.49×10^2
PS 0.1	105	0.026	-54	5.78×10^1	3.35×10^3	1.94×10^5
PS 0.05	59	0.128	-51	1.03×10^2	1.06×10^4	1.09×10^6

Results for the polystyrene particle clearance are shown in Figure 19. An effect on mucociliary particle clearance was most presumable to occur for the 50 nm polystyrene particles since, comparing 6000 nm and 50 nm spheres, particle

diameter [d], surface [A], and number [N] differed by a factor of $f_d = 1.03 \times 10^2$, $f_A = 1.06 \times 10^4$, and $f_N = 1.09 \times 10^6$, respectively. Interestingly, the mucociliary transport rates (MTR) of differently sized polystyrene particles did not differ significantly ($P < 0.05$). MTR were found to be (3.2 ± 0.6) mm/min for 6000 nm particles, (3.8 ± 0.8) mm/min for 1000 nm particles, (3.8 ± 0.9) mm/min for 100 nm particles, and (2.9 ± 0.6) mm/min for 50 nm particles, suggesting that particle size does not appear to be a primary or critical factor for mucociliary particle clearance.

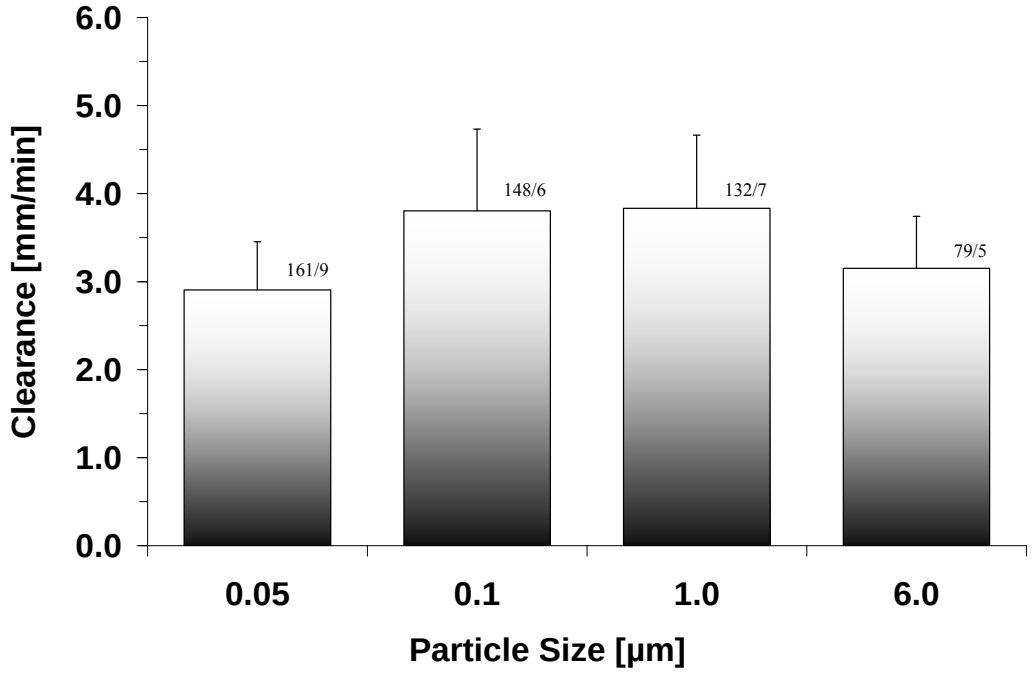

Figure 19: Clearance of Different-Sized Polystyrene (PS) Particles

Results (mean ± SD) for polystyrene particle transport rates [mm/min] as determined from the clearance experiments. Numbers beside the bars designate the numbers of particles/tracheas investigated. Mucociliary transport rates (MTR) of different-sized polystyrene particles were not found to be significantly different ($P < 0.05$).

6.4.2. Influence of Particle Surface Properties

Results from the clearance experiments of the polymeric nanoparticles are shown in Figure 20. Mucociliary transport rates (MTR) of the different polymeric particles were significantly different. Results of particle characterization were as expected according to the polymers chemical structure (Table 3). Particle size and zeta potential ranged between 90 nm to 400 nm, and -42 mV to +47 mV, respectively.

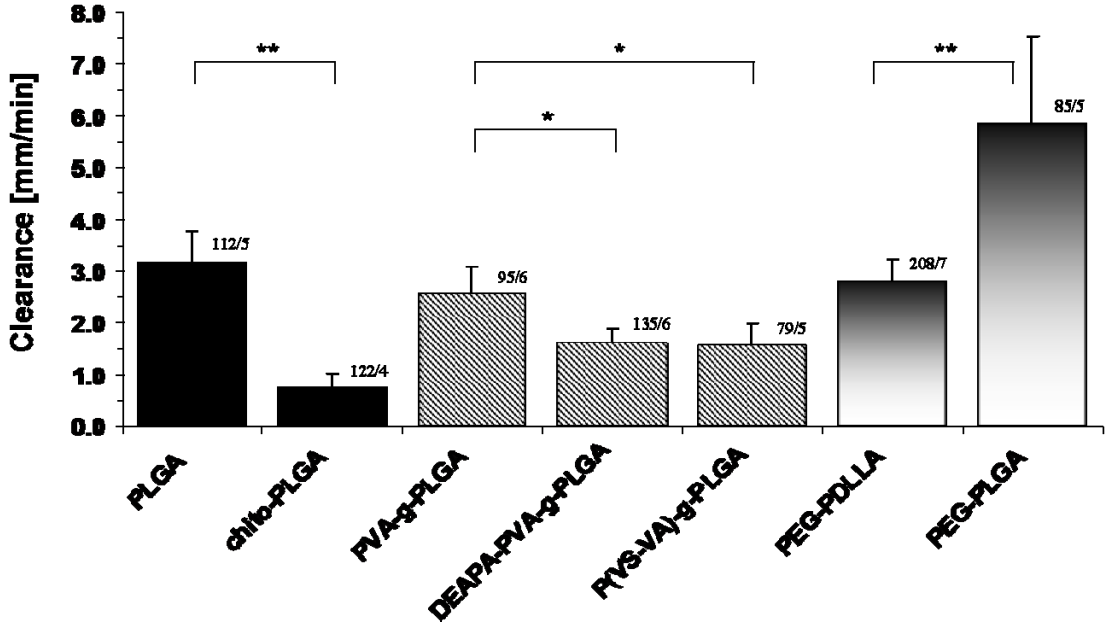

Figure 20: Clearance of Different Polymeric Particles

Results (mean ± SD) for particle transport rates [mm/min] as determined from the *in vitro* clearance experiments. Numbers beside the bars designate the numbers of particles investigated, e.g., "100/5" indicates 100 particles tracked on 5 tracheas. Transport rates of different polymeric particles show no significant difference (* $P < 0.01$; ** $P < 0.001$).

Table 3: Results of Polymeric Particle Characterization

Results of particle characterization were as expected according to the polymers chemical structure. Particle diameter (d), polydispersity index (PDI), zeta-potential (Zeta), mucociliary transport rates (MTR).

Particles	Diameter [nm]	PDI [-]	Zeta [mV]	MTR [mm/min]
PLGA	157	0.043	-10	3.2 ± 0.6
chitosan-PLGA	163	0.052	18	0.7 ± 0.3
PVA-g-PLGA	127	0.076	-40	2.6 ± 0.5
DEAPA-PVA-g-PLGA	92	0.271	47	1.6 ± 0.3
P(VS-VA)-g-PLGA	142	0.059	-43	1.6 ± 0.4
PEG-PDLLA	82	0.167	-21	2.8 ±0.4
PEG-PLGA	389	0.151	-16	5.9 ±1.7

Polymers I and II:

MTR of equally sized PLGA (I) and chitosan-PLGA (II) particles were (3.2 ± 0.6) mm/min and (0.7 ± 0.3) mm/min, respectively. In comparison with blank PLGA (I) particles, this corresponds to a considerable reduction of chitosan-PLGA (II) particle clearance by a factor of 4-5. Clearance rates of PLGA (I) particles and similarly sized 100 nm polystyrene particles (PS 0.1) were comparable: (3.2 ± 0.6) mm/min vs. (3.8 ± 0.9) mm/min, which supports the outcome of the polystyrene particle experiments. Zeta-potential of the particles was according to the materials' chemical structures (Table 3); a positive zeta-potential, induced by the primary amine-groups present within the chitosan polysaccharide structure, was determined for chitosan-PLGA (II) particles. Blank PLGA (I) nanospheres exhibited a negative zeta-potential due to the prevailing acidic structure of the polymer.

Polymers III-V:

Clearance rates of PVA-g-PLGA (III), DEAPA-PVA-g-PLGA (IV), and P(VS-VA)-g-PLGA (V) were (2.6 ± 0.5) mm/min, (1.6 ± 0.3) mm/min, and (1.6 ± 0.4) mm/min, respectively. Both DEAPA-PVA-g-PLGA (IV) and P(VS-VA)-g-PLGA (V) particles were transported significant slower than PVA-g-PLGA (III) particles, considered as the lead polymeric structure in this experimental polymer group (Table 1, Annex A.2). In parallel to chitosan-PLGA (II), the DEAPA-PVA-g-PLGA (IV) includes amine functions within the polymer structure, resulting in a positive zeta-potential of the DEAPA-PVA-g-PLGA (IV) particles. Comparing PVA-g-PLGA (III) and P(VS-VA)-g-PLGA (V) particles, no amine groups were present in these polymers. Size and zeta-potential for both PVA-g-PLGA (III) and P(VS-VA)-g-PLGA (V) particles was comparable and highly negative. Thus differences in particle MTR are presumably based on the polymers' chemical structure.

Polymers VI and VII:

Surprisingly, clearance rates for PEG-PDLLA (VI) and PEG-PLGA (VII) particles were significantly different, although the particles' zeta-potential values and polymer structures are comparable at first glance (Table 1, Annex A.2). The clearance rate of PEG-PDLLA (VI) particles was (2.8 ± 0.4) mm/min, whereas PEG-PLGA (VII) particles were transported at a rate of (5.9 ± 1.7) mm/min. Focusing more detailed on the polymers' structure it became clear that the main difference was the molecular weight (MW) of the polyethylenglycol (PEG) used in the polymer synthesis: A high molecular weight PEG (10kDa) was employed for the PEG-PDLLA (VI) synthesis, whereas a low molecular weight PEG (5 kDa) was used for PEG-PLGA (VII). Therefore, it is suggested that mucociliary clearance for PEG-PDLLA (VI) and PEG-PLGA (VII) particles mainly reflects influences based on the different PEG qualities.

6.5. Discussion

It can be expected that molecular weight, chemical structure, charge, and the dimensional texture of a molecule have major influences on its interactions with and clearance from the human body. However, to what extent these factors may also affect mucociliary clearance had not been investigated previously. In view of the average tracheal clearance velocity, as determined by noninvasive radiological techniques in healthy non-smokers, mucociliary clearance varied between 4.0 and 6.0 mm/min (Hofmann and Asgharian, 2003). Based on these results, the International Commission on Radiological Protection (ICRP) and the National Council on Radiological Protection (NCRP) adopted an average tracheal clearance velocity of 5.5 mm/min (ICRP, 1994; NCRP, 1997). Considering our results for particle clearance, the trachea-based *in vitro* model showed the fastest or "normal" mucociliary transport rates (~6.0 mm/min) with the PEG-PLGA (VII) particles. However, the transport rates of other polymeric nanoparticles varied significantly, as discussed below.

6.5.1. Particle Size and Correlated Factors

By today several studies were carried out to clarify the underlying mechanisms of long-term particle clearance (>24h) from the airways. As yet, particle size has been proposed to contribute to this clearance phenomenon (Scheuch and Stahlhofen, 1987; Stahlhofen et al., 1986; Stahlhofen et al., 1990). Though it could not be excluded that long-term clearance in these studies occurred due to particle deposition in the deep lung, where rapid particle clearance by the mucociliary elevator is not present.

In our study, taking the clear advantage that alveolar deposition can be excluded in a trachea-based model per se, our first attempt was to investigate the influence of particle size, surface, and number on mucociliary particle clearance. According to theory a higher number of particles as well as a larger particle surface inevitably

results in a higher chance for mucus-particle interactions. Previously we assumed that, comparing 50 nm and 6000 nm particles and differences in particle size, total surface, and total number, the 50 nm particles have a much higher chance to influence mucociliary particle clearance and to interact with the mucin network. However, mucociliary transport rates for 50 nm up to 6000 nm sized polystyrene particles did not differ significantly even though particle size, surface and number varied tremendously by several orders of magnitude. Considering the overall results of mucociliary particle clearance, there was no conclusive correlation (R^2) of clearance rates and particle size (d), surface (A), or volume (V): $R_d^2 = 0.1712$, $R_A^2 = 0.1061$, $R_V^2 = 0.0738$. Hence, at this point it seems that particle properties other than size and correlated factors primarily affect airway particle clearance and long-term clearance, respectively.

6.5.2. Particle Surface Properties

The second objective was to investigate the effect of particle surface characteristics, determined by the materials' chemical structure, on mucociliary particle clearance. Previously it was shown that polysaccharides and acrylic acids are capable to affect mucociliary clearance rates by changing the viscoelastic properties of the mucus (Shah and Donovan, 2007a, b). Here, we assumed that mucoadhesive properties and the zeta-potential of particles may also affect particle clearance velocity.

Chitosan particles:

Over the last two decades, chitosan has been used for various biomedical and drug delivery applications due to its biocompatibility, mucoadhesive properties and slight antimicrobial effects (Agnihotri et al., 2004; Lehr, 2000; Rabea et al., 2003). Mucoadhesive properties of chitosan particles are predominantly based on electrostatic attraction of primary amine groups present within the polysaccharide structure of chitosan (Sogias et al., 2008). In theory, strongly mucoadhesive particles

will be captured directly on top of the mucus layer, since penetration into the mucus layer is inhibited by particle adhesion to the outermost located mucins of the mucus layer. Interestingly, the chitosan-PLGA (II) particles were transported 4-5 times slower than the blank PLGA (I) nanospheres (Figure 20), although rapid immobilization on top of the mucus layer should result in spatially limited effects on mucociliary clearance. It is supposed that chitosan-PLGA (II) particles were either able to penetrate into the mucus layer, or the extent of mucus-particle interaction, even on top of the mucus layer, considerably changed the overall mucus transport properties. Here, fractional penetration of ~160 nm sized chitosan-PLGA (II) particles into the mucus layer seems to be reasonable, since rapid mucus penetration was also reported for considerably bigger (500 nm) particles (Lai et al., 2007).

PEG-Particles:

Mucociliary clearance rates for PEG-PDLLA (VI) and PEG-PLGA (VII) particles were significantly different although the zeta-potential values and polymer structures are comparable (Figure 20, Table 2). Focusing on the polymer structure, a clear difference is the PEG used in the polymer synthesis: A high molecular weight PEG (10 kDa) was used for PEG-PDLLA (VI) synthesis, whereas low molecular weight PEG (5 kDa) was used in the PEG-PLGA (VII).

Previously it has been demonstrated that PEG molecular weight can significantly affect mucin-particle interaction by interpenetration of PEG-chains into the mucus network. Huang et al. (Huang et al., 2000) reported mucoadhesive PEG properties for high molecular weight PEG (> 10 kDa), whereas Lai et al. (Lai et al., 2007) could show strongly reduced mucoadhesive interaction for low molecular weight PEG (< 2kDa) nanoparticles. Generally, PEG_{10kDa}-PDLLA (VI) can be described as a di-block copolymer, whereas PEG_{5kDa}-PLGA (VII) is a tri-block copolymer. From this structural aspect, the 10kDa PEG-block in the di-block copolymer per se is located at a higher ratio at the polymer-mucus interface, and thus has a higher probability to interact with the mucus network. On the other hand but due to the same structural

aspects, the 5kDa PEG-block within the PEG_{5kDa}-PLGA (VII) tri-block has a lower potential to interact with the inner mucus structure. Therefore, differences between mucociliary particle clearance of PEG_{10kDa}-PDLLA (VI) and PEG_{5kDa}-PLGA (VII) particles presumably reflect the differences in mucus-particle interaction of the PEG polymers as is sketched in Figure 21.

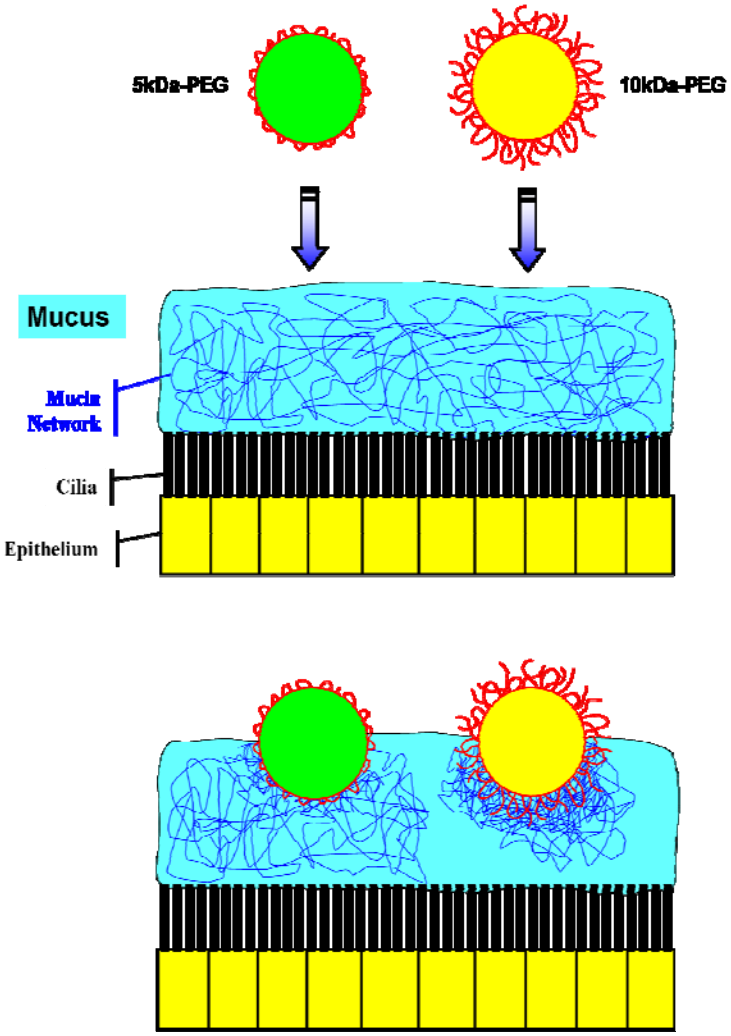

Figure 21: Exemplary Scheme of PEG-Mucus Interaction

The scheme shows the mucus layer and the incorporated mucin network A) prior, and B) after deposition of PEG-co-polymeric particles. A higher degree of PEG-chain interpenetration into the mucin network, as can be assumed for the 10kDa PEG-di-block particles, will influence the inner mucus structure and transport properties more significantly.

Looking at the clearance rates of PEG_{5kDa}-PLGA (VII) versus blank PLGA (I) particles, this interpretation is even more corroborated since also the blank PLGA (I) particles exhibit a significantly reduced MTR in comparison to the PEG_{5kDa}-PLGA (VII) particles. With respect to the potential influence of PDLLA vs. PLGA, a certain influence on particle transport might be assumed, but due to the results reported seems unlikely to be of significant importance here.

Zeta-potential and chemical particle structure:

In parallel to particle size, no reasonable correlation between zeta potential and mucociliary particle clearance could be observed (Figure 22). Overall correlation (R^2) of zeta-potential and particle clearance was ($R^2 = 0.1762$).

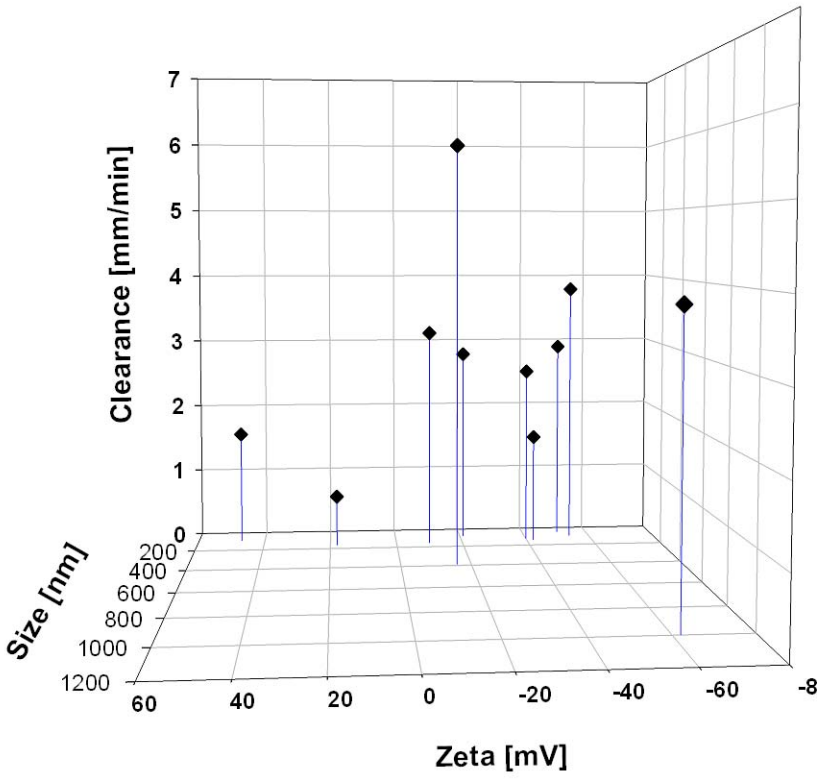

Figure 22: 3D-Plot of Particle Size, Zeta-Potential, and Mucociliary Clearance

For the different polymeric particles tested in this study, no reasonable correlation between particle size, zeta potential, and mucociliary particle clearance could be observed.

Though, looking at the chemical structure of the polymers (Table 2, Annex A.2), similar findings can be drawn as for the chitosan-PLGA (II) particles: In parallel to the mucoadhesive chitosan-PLGA (II), the DEAPA-PVA-g-PLGA (IV) also includes amine functions within the polymer structure. Consequently, the electrostatic interplay of mucus and DEAPA-PVA-g-PLGA (IV) particles is likely to be the reason for reduced particle clearance, too. Less efficient reduction of DEAPA-PVA-g-PLGA (IV) particle transport, as compared to chitosan-PLGA (II) particles, might occur due to sterical reasons: the DEAPA's tertiary amine function may hinder the electrostatic interaction to a higher extent than primary amine groups present in chitosan.

Comparing PVA-g-PLGA (III) and P(VS-VA)-g-PLGA (V) particles, no amine groups were present in these polymers. Size and the zeta potential values for both PVA-g-PLGA (III) and P(VS-VA)-g-PLGA (V) particles were comparable and highly negative. Thus, significant differences in particle clearance may be based on differences in the polymers' chemical structures, i.e. the vinylsulfonate (VS) groups in the P(VS-VA)-g-PLGA particles. In general vinylsulfonate groups exhibit potent H-bond acceptor qualities, which might be the source of interaction with the highly glycosylated mucins of the mucus layer and resulting differences in mucociliary clearance rates.

6.6. Conclusion

Although there is a huge variety of application devices and drugs available, pneumology specialists agree on insufficient therapeutic standards regarding duration of drug effects and regional targeting within the respiratory system. In this context, mucociliary clearance acts as a major problem limiting the benefit of most inhalation therapies. Once the drug particles entered and deposited within the airways, mucociliary clearance immediately removes the particles from the intended target site. By today the most significant parameters for mucociliary particle clearance are not fully understood and still are under debate. Considering our results for *in vitro* mucociliary particle clearance and correlations with physico-chemical particle properties, several findings seem to be evident:

1) **Size and zeta-potential seem to be minor critical factors for mucociliary particle clearance, which could be shown for polystyrene as well as different polymeric nanoparticles covering a broad size and zeta-potential range.**

2) **Interestingly, the chemical surface structure of the particles was found to be a most important factor for mucociliary particle clearance, offering possibilities to achieve faster or slower particle clearance.**

In the case of chitosan-PLGA and DEAPA-PVA-g-PLGA particles, the number and dimensional latitude of amine functions seem to affect particle clearance. These findings once more underline that chitosan and similar chemical modifications may be used if therapeutic interventions include beneficial effects due to adhesive interaction between the drug-carrier system and the mucosal barrier. For polyethylenglycol-copolymers, mucociliary particle clearance seems to be effected by the PEG's molecular weight: PEG_{10kDa}-PDLLA particles showed reduced particle clearance, whereas PEG_{5kDa}-PLGA particles were cleared at normal transport rates, compared to

the ICRP's standard value for average tracheal clearance rates. Although mucociliary clearance comprises a more complex situation than the systems studied by Huang et al. (Huang et al., 2000) or Lai et al. (Lai et al., 2007), the outcome of previous studies strongly support the experimental results presented here. At this point the demand for detailed investigations of mucus-particle and mucus-drug interactions to elucidate changes in the mucin network shall be clearly emphasized. With regard to the overall results from this study, a new and more concrete pulmonary drug delivery approach may be defined as:

The ideal drug or drug loaded carrier system should be able to escape from mucociliary clearance if there are no or only minimal interactions with the mucus layer. Thereby the chance of rapid penetration into the periciliary layer, located underneath the mucus, is increased and interaction of the drug or carrier with the airway epithelium is more likely to occur.

7. Overall Conclusion and Outlook

According to the World Health Organization (WHO) approximately 300 million people currently have asthma, and its prevalence increases by 50% every decade. Moreover, the WHO predicts Chronic Obstructive Pulmonary Disease (COPD) to become the 3rd leading cause of death by 2030 (WHO, 2008). Based on these facts it seems to be highly desirable to improve therapeutic options for inhalation therapy, currently strongly limited by the efficient lung clearance mechanisms. Moreover, designing pulmonary drug formulations, one should generally consider potential interactions with the mucus layer and mucociliary clearance as a key factor for therapeutic success of the delivery concept.

In this context the ECT clearance model represents a valuable tool comprising scientific, economic, and ethical advantages to investigate mucociliary lung clearance and related topics. A most important result from the work presented is that the chemical surface structure of particles significantly influences mucociliary particle clearance, whereas particle size seems to act as a less critical factor. Here, in terms of risk assessment as well as basic research, further experiments employing a larger number of chemically defined particles may help to elucidate on critical chemical parameters for mucociliary particle clearance. Future experiments aiming to understand the fate of particles after interaction or penetration into the mucus network seem to be a major demand as it is not clear if the mucin network is a robust or highly delicate factor for functional mucus clearance. Further investigations on mucin-particle interaction at the bulk- as well as microrheological level as well as microscopic studies are needed.

With respect to the EU's REACH initiative, the findings in this work underline the need for additional pulmonary risk assessment. Many inhalable micro- and nanosized materials were and still are employed in industrial manufacturing processes. These

materials often exhibit size-dependent physico-chemical properties and hence should be considered for more detailed investigation of airway particle clearance and toxicological effects. In this context employment of the ECT *in vitro* model can help to realize the '3R' concept (Reduce, Refine, and Replace) in animal experiments, which was first stated in 1959 (Russel and Burch, 1959) and till today is strongly supported by the German ZEBET[1] as well as international authorities like the ECVAM[2].

[1] Zentralstelle zur Erfassung und Bewertung von Ersatz- und Ergänzungsmethoden zum Tierversuch (ZEBET)

[2] European Centre for the Validation of Alternative Methods (ECVAM)

8. Annex

A.1 Exemplary Image Sequence of Mucociliary Particle Clearance

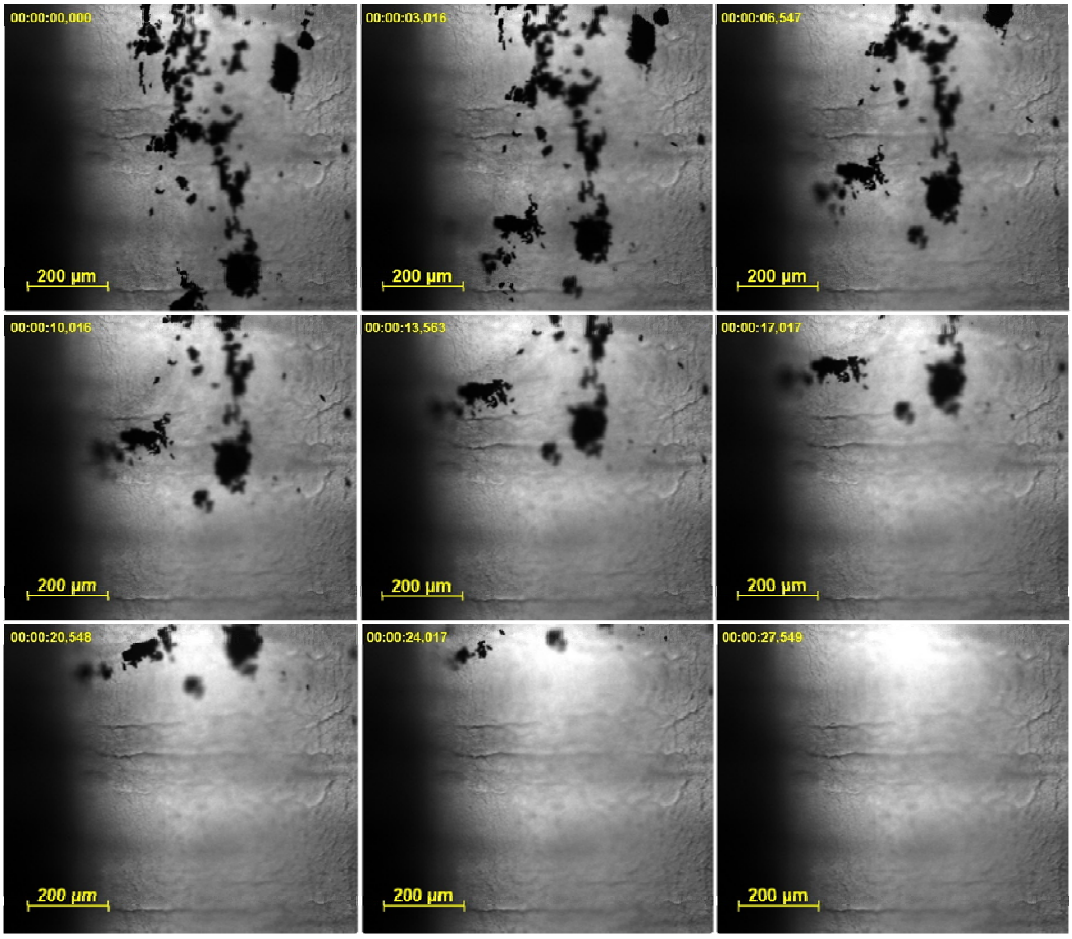

After deposition on the tracheal surface, carbon particles were only transported into proximal direction, i.e. towards the upper end of the trachea. As can be seen from the sequence, mucociliary clearance efficiently clears all carbon particles from the tracheal surface. The image sequence above shows 9 pictures, selected from a total of 60 pictures, generated during a carbon particle clearance experiment. The course of time is represented from left to right as is also indicated by the relative time displayed in each image. Particle imaging was realized via transmission light microscopy (top-view). Blurry regions in the middle of each picture result from depth of focus, a technical limitation given by the technical dimensions of each microscope objective.

A.2 Chemical Structure of Mono- and Polymers

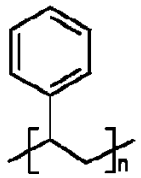 Polystyrene	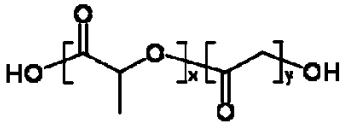 Poly-(lactide-co-glycolide)	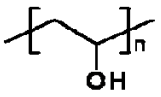 Poly-(vinyl alcohol)
 Poly-(ethylen glycol)	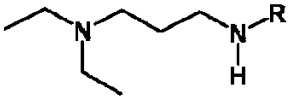 DEAPA (Diethylaminopropyl amine)	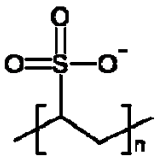 Poly-(vinyl sulfonate)
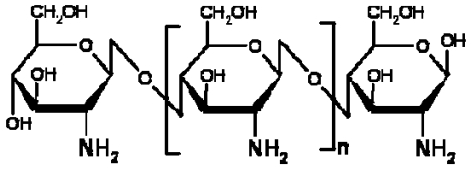 Chitosan (Poly-ß-(1-4)-D-Glucosamin)		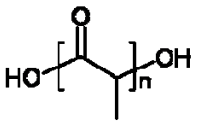 Poly-(lactide)

The table shows basic structures of all polymers employed in the particle clearance experiments. Chitosan and DEAPA structure includes primary and tertiary amine functions, respectively. Considering sterical aspects, the DEAPA's tertiary amine function is shielded by ethyl groups which may be the reason for faster mucociliary clearance for DEAPA- as compared to chitosan-co-polymeric particles.

A.3 Experimental Set-up

A) Microscope Set-up

In order to realize mucociliary clearance experiments at different temperature and humidity levels, the upright microscope was fully integrated in a polycarbonate box, customized by LIS (Life Imaging Services, Reinach, CH).

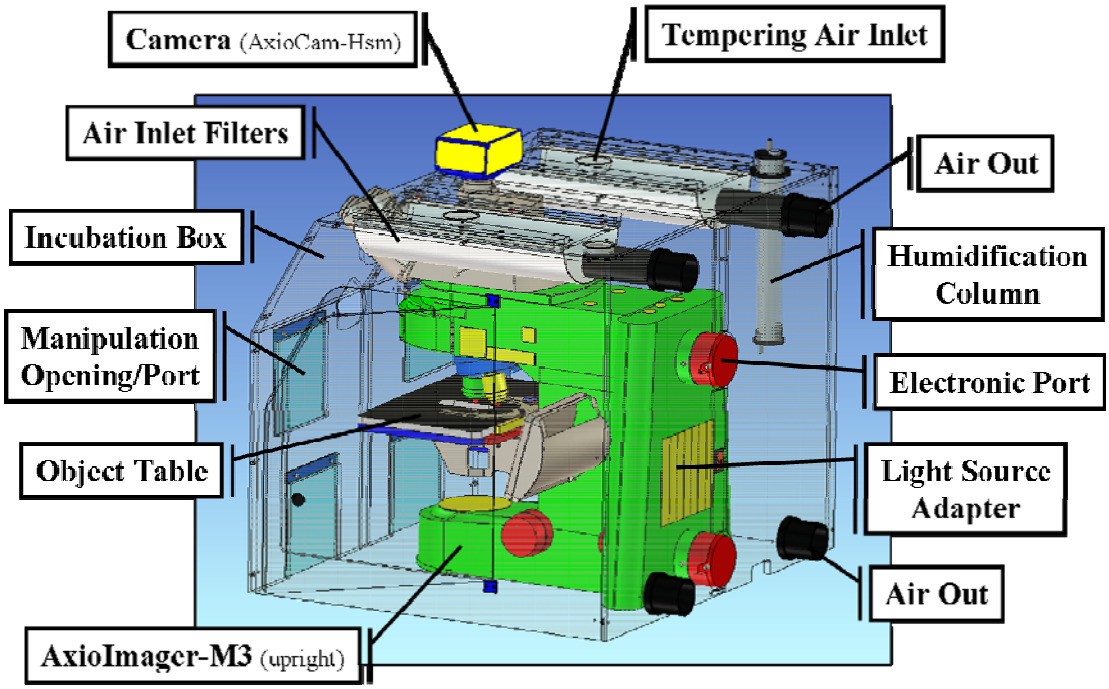

During the tracking experiments the microscope could be operated either manually or fully automated via the computer interface. Insulating properties of the overall Set-up were studied in order to ensure constant temperature and humidity levels during the particle clearance experiments. From these results *(see 5.4.2. Validation of the Experimental Set-up)* a general lead time could be defined to provide stable and defined experimental conditions. Illumination of particles was realized using either mercury vapor or LED technology (Colibri, ZEISS, Germany) as fluorescence light source, depending on imaging properties of the particles.

B) Incubation chamber

The picture shows all individual parts of the incubation chamber, customized by LIS (Life Imaging Services, Reinach, CH). Subsequently, after the test particles were deposited on the tracheal surface, the chamber was closed via the magnetic seal. Different humidity levels in the closed chamber were realized by induction of a preconditioned airflow at the left side of the Teflon ring (a), placed between top (c) and base plate (b). During the validation experiments (*5.4.2., page 34*) the progression of temperature and relative humidity was measured directly in outlet airflow (right). To avoid fogging of the glass windows during the tracking experiments, the glass surface was modified using octadecyltrichlorosilane (OTS). S*ee also 5.3.3., page 29*.

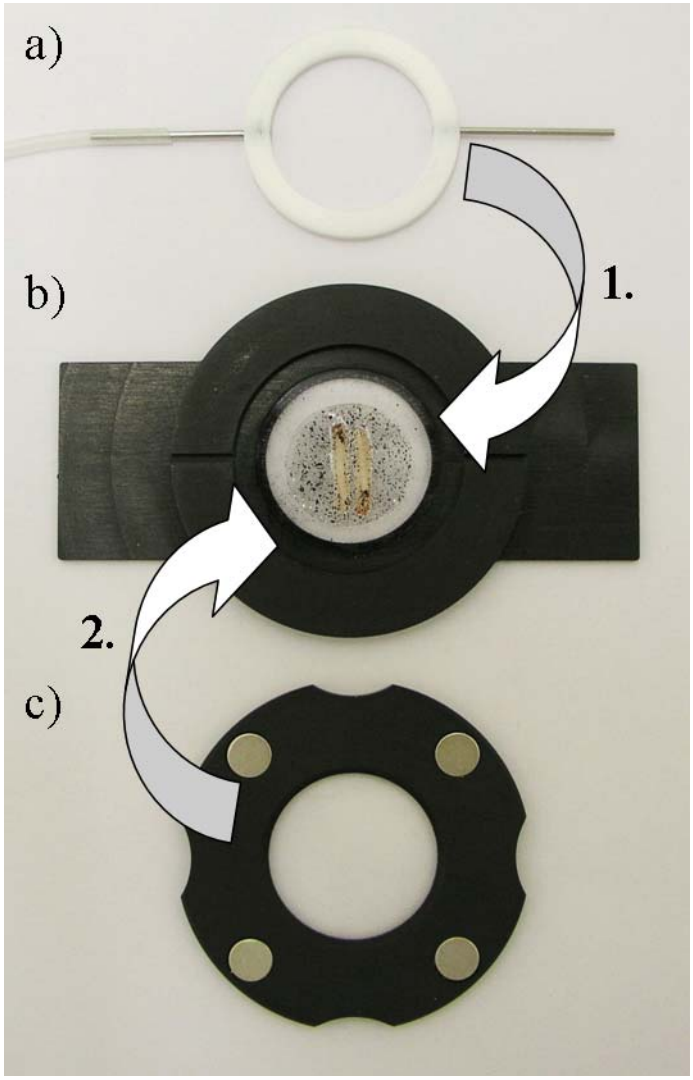

9. List of Abbreviations

AT-I/II	Alveolar type I/II cells
ATP	Adenosine triphosphate
BCA	Bicinchoninic acid
cAMP	Cyclic adenosine monophosphate
CBF	Ciliary beat frequency
CF	Cystic fibrosis
COPD	Chronic obstructive pulmonary disease
ECT	Embryonic chicken trachea
ECVAM	European Centre for the Validation of Alternative Methods
ICRP	International Commission on Radiological Protection
MC	Mucociliary clearance
MTR	Mucociliary transport rate
MUC*x*	Mucin *x* encoding gene
NAC	N-Acetylcysteine
NCRP	National Council on Radiological Protection
OTS	Octadecyltrichlorosilane
PAGE	Polyacrylamide gel electrophoresis
PCL	Periciliary layer
PDD	Pulmonary drug delivery
PDI	Polydispersity index
PM	Particulate matter
RPM	Rounds per minute
SDS	Sodium dodecyl sulfate
SEM	Scanning electron microscopy
SP-A	Surfactant protein A
SPF	Specific pathogen free

TEM	Transmission electron microscopy
UFP	Ultra fine particles
WHO	World Health Organization
ZEBET	Zentralstelle zur Erfassung und Bewertung von Ersatz- und Ergänzungsmethoden zum Tierversuch

Polymer abbreviations see 6.2, page 52.

10. References

Afzelius BA (2000) Ciliary structure in health and disease. Acta Oto-Rhino-Laryngologica Belgica 54: 287-291.

Agnihotri SA, Mallikarjuna NN, Aminabhavi TM (2004) Recent advances on chitosan-based micro- and nanoparticles in drug delivery. Journal of Controlled Release 100: 5-28.

Aiache JM (1990) Aerosol therapy in France. Journal of Aerosol Medicine: Deposition, Clearance, and Effects in the Lung: 85–120.

Albertine KH, Williams MC, Hyde DM (2000) Anatomy and development of the respiratory tract. In: Murray JF, Nadel JA (eds) Textbook of respiratory medicine. W.B. Saunders CBS Educ. and Professional Publ., New York, NY, pp 3-33.

Amin RS, Wert SE, Baughman RP, Tomashefski Jr JF, Nogee LM, Brody AS, Hull WM, Whitsett JA (2001) Surfactant protein deficiency in familial interstitial lung disease. Journal of Pediatrics 139: 85-92.

Annesi-Maesano I, Forastiere F, Kunzli N, Brunekref B (2007) Particulate matter, science and EU policy. European Respiratory Journal 29: 428-431.

Bennet C (1654) *Theatri tabidorum vestibulum: seu exercitationes dianoeticae cum historiis et experimentis demonstratives*. Newcomb, London, pp 1-126.

Bennett WD, Scheuch G, Zeman KL, Brown JS, Kim C, Heyder J, Stahlhofen W (1999) Regional deposition and retention of particles in shallow, inhaled boluses: Effect of lung volume. Journal of Applied Physiology 86: 168-173.

Bivas-Benita M, Ottenhoff THM, Junginger HE, Borchard G (2005) Pulmonary DNA vaccination: Concepts, possibilities and perspectives. Journal of Controlled Release 107: 1-29.

Blake JR, Sleigh MA (1974) Mechanics of ciliary locomotion. Biological Reviews of the Cambridge Philosophical Society 49: 85-125.

Blank F, Rothen-Rutishauser BM, Schurch S, Gehr P (2006) An optimized *in vitro* model of the respiratory tract wall to study particle cell interactions. Journal of Aerosol Medicine: Deposition, Clearance, and Effects in the Lung 19: 392-405.

Boek WM, Romeijn SG, Graamans K, Verhoef JC, Merkus FWHM, Huizing EH (1999a) Validation of animal experiments on ciliary function *in vitro*. I. The influence of substances used clinically. Acta Oto-Laryngologica 119: 93-97.

Boek WM, Romeijn SG, Graamans K, Verhoef JC, Merkus FWHM, Huizing EH (1999b) Validation of animal experiments on ciliary function *in vitro*. II. The influence of absorption enhancers, preservatives and physiologic saline. Acta Oto-Laryngologica 119: 98-101.

Booker R (2005) Do patients think that dry powder inhalers can be used interchangeably? International Journal of Clinical Practice 59: 30-32.

Bousquet J, Dahl R, Khaltaev N (2007) Global Alliance against Chronic Respiratory Diseases. European Respiratory Journal 29: 233-239.

Brand P, Friemel I, Meyer T, Schulz H, Heyder J, Huinger K (2000) Total deposition of therapeutic particles during spontaneous and controlled inhalations. Journal of Pharmaceutical Sciences 89: 724-731.

Brand P, Rieger C, Beinert T, Heyder J (1995) Aerosol derived airway morphometry in healthy subjects. European Respiratory Journal 8: 1639-1646.

Brown JS, Bennett WD (2004) Deposition of coarse particles in cystic fibrosis: Model predictions versus experimental results. Journal of Aerosol Medicine: Deposition, Clearance, and Effects in the Lung 17: 239-248.

Clary-Meinesz CF, Cosson J, Huitorel P, Blaive B (1992) Temperature effect on the ciliary beat frequency of human nasal and tracheal ciliated cells. Biology of the Cell 76: 335-338.

Corkery K (2000) Inhalable drugs for systemic therapy. Respiratory Care 45: 831-835.

Dessanges JF (2001) A history of nebulization. Journal of Aerosol Medicine: Deposition, Clearance, and Effects in the Lung 14: 65-71.

Desseyn JL, Aubert JP, Porchet N, Laine A (2000) Evolution of the large secreted gel-forming mucins. Molecular Biology and Evolution 17: 1175-1184.

Dhand R (2005) Aerosol plumes: Slow and steady wins the race. Journal of Aerosol Medicine: Deposition, Clearance, and Effects in the Lung 18: 261-263.

Dolovich MA, MacIntyre NR, Anderson PJ, Camargo C.A, Jr., Chew N, Cole CH, Dhand R, Fink JB, Gross NJ, Hess DR, Hickey AJ, Kim CS, Martonen TB, Pierson DJ, Rubin BK, Smaldone GC (2000) Consensus statement: Aerosols and delivery devices. Respiratory Care 45: 589-596.

Dominici F, Peng RD, Bell ML, Pham L, McDermott A, Zeger SL, Samet JM (2006) Fine particulate air pollution and hospital admission for cardiovascular and respiratory diseases. Journal of the American Medical Association 295: 1127-1134.

Felicetti SA, Wolff RK, Muggenburg BA (1981) Comparison of tracheal mucous transport in rats, guinea pigs, rabbits, and dogs. Journal of Applied Physiology Respiratory Environmental and Exercise Physiology 51: 1612-1617.

Forbes B (2002) Pulmonary epithelial cell culture. Methods in molecular biology (Clifton, N.J.) 188: 65-75.

Forbes B, Ehrhardt C (2005) Human respiratory epithelial cell culture for drug delivery applications. European Journal of Pharmaceutics and Biopharmaceutics 60: 193-205.

Foster WM, Langenback E, Bergofsky EH (1980) Measurement of tracheal and bronchial mucus velocities in man: Relation to lung clearance. Journal of Applied Physiology Respiratory Environmental and Exercise Physiology 48: 965-971.

Foster WM, Langenback EG, Bergofsky EH (1982) Lung mucociliary function in man: Interdependence of bronchial and tracheal mucus transport velocities with lung clearance in bronchial asthma and healthy subjects. Annals of Occupational Hygiene 26: 227-244.

Fuloria M, Rubin BK (2000) Evaluating the efficacy of mucoactive aerosol therapy. Respiratory Care 45: 868-873.

Ganachaud F, Katz JL (2005) Nanoparticles and nanocapsules created using the ouzo effect: Spontaneous emulsification as an alternative to ultrasonic and high-shear devices. European Journal of Chemical Physics and Physical Chemistry 6: 209-216.

Gehr P, Bachofen M, Weibel ER (1978) The normal human lung: ultrastructure and morphometric estimation of diffusion capacity. Respiration Physiology 32: 121-140.

Gehr P, Geiser M, Hof VI, Schurch S, Waber U, Baumann M (1993) Surfactant and inhaled particles in the conducting airways: Structural, stereological, and biophysical aspects. Microscopy Research and Technique 26: 423-436.

Gehr P, Green FHY, Geiser M, Im Hof V, Lee MM, Schürch S (1996) Airway surfactant, a primary defense barrier: Mechanical and immunological aspects. Journal of Aerosol Medicine: Deposition, Clearance, and Effects in the Lung 9: 163-181.

Geiser M, Gerber P, Maye I, Im Hof V, Gehr P (2000) Retention of Teflon particles in hamster lungs: A stereological study. Journal of Aerosol Medicine: Deposition, Clearance, and Effects in the Lung 13: 43-55.

Geiser M, Rothen-Rutishauser B, Kapp N, Schu?rch S, Kreyling W, Schulz H, Semmler M, Im Hof V, Heyder J, Gehr P (2005) Ultrafine particles cross cellular membranes by nonphagocytic mechanisms in lungs and in cultured cells. Environmental Health Perspectives 113: 1555-1560.

Gerber V, Gehr P, Straub R, Frenz M, King M, Im Hof V (1997) Mucus quality on horse tracheal epithelium: Microscopic grading based on transparency. Respiration Physiology 107: 67-74.

Grafahrend D, Calvet JL, Klinkhammer K, Salber J, Dalton PD, Möller M, Klee D (2008) Control of protein adsorption on functionalized electrospun fibers. Biotechnology and Bioengineering 101: 609-621.

Gray T, Koo JS, Nettesheim P (2001) Regulation of mucous differentiation and mucin gene expression in the tracheobronchial epithelium. Toxicology 160: 35-46.

Groneberg DA, Eynott PR, Lim S, Oates T, Wu R, Carlstedt I, Roberts P, McCann B, Nicholson AG, Harrison BD, Chung KF (2002a) Expression of respiratory mucins in fatal status asthmaticus and mild asthma. Histopathology 40: 367-373.

Groneberg DA, Eynott PR, Oates T, Lim S, Wu R, Carlstedt I, Nicholson AG, Chung KF (2002b) Expression of MUC5AC and MUC5B mucins in normal and cystic fibrosis lung. Respiratory Medicine 96: 81-86.

Groneberg DA, Witt C, Wagner U, Chung KF, Fischer A (2003) Fundamentals of pulmonary drug delivery. Respiratory Medicine 97: 382-387.

Haagsman HP, Diemel RV (2001) Surfactant-associated proteins: Functions and structural variation. Comparative Biochemistry and Physiology - A Molecular and Integrative Physiology 129: 91-108.

Hawgood S (1997) Surfactant: Composition, structure, and metabolism. In: Crystal RG, West JB, Weibel ER, Barnes PJ (eds) The Lung: Scientific Foundations. Lippincott–Raven, Philadelphia., pp 557-571.

Hermans C, Bernard A (1999) Lung epithelium-specific proteins: Characteristics and potential applications as markers. American Journal of Respiratory and Critical Care Medicine 159: 648-678.

Heyder J (1981) Mechanisms of aerosol particle deposition. Chest 80: 820-823.

Heyder J, Gebhart J, Rudolf G, Schiller CF, Stahlhofen W (1986) Deposition of particles in the human respiratory tract in the size range 0.005-15 μm. Journal of Aerosol Science 17: 811-825.

Heyder J, Svartengren MU (2002) Basic principles of particle behavior in the human respiratory tract. Drug Delivery to the Lung: 21-45.

Hochrainer D, Hoelz H, Kreher C, Scaffidi L, Spallek M, Wachtel H (2005) Comparison of the aerosol velocity and spray duration of Respimat® Soft Mist™ inhaler and pressurized metered dose inhalers. Journal of Aerosol Medicine: Deposition, Clearance, and Effects in the Lung 18: 273-282.

Hofmann W, Asgharian B (2003) The effect of lung structure on mucociliary clearance and particle retention in human and rat lungs. Toxicological Sciences 73: 448-456.

Horisawa E, Kubota K, Tuboi I, Sato K, Yamamoto H, Takeuchi H, Kawashima Y (2002) Size-dependency of DL-lactide/glycolide copolymer particulates for intra-articular delivery system on phagocytosis in rat synovium. Pharmaceutical Research 19: 132-139.

Huang Y, Leobandung W, Foss A, Peppas NA (2000) Molecular aspects of muco- and bioadhesion: Tethered structures and site-specific surfaces. Journal of Controlled Release 65: 63-71.

ICRP (1994) Human respiratory tract model for radiological protection. Annals of the International Commission on Radiological Protection 24: 1-120.

Iravani J, As van A (1972) Mucus transport in the tracheobronchial tree of normal and bronchitic rats. Journal of Pathology 106: 81-93.

King M (1979) Interrelation between mechanical properties of mucus and mucociliary transport: Effect of pharmacologic interventions. Biorheology 16: 57-68.

King M (1980) Relationship between mucus viscoelasticity and ciliary transport in guaran gel/frog palate model system. Biorheology 17: 249-254.

King M (1998) Experimental models for studying mucociliary clearance. European Respiratory Journal 11: 222-228.

Kirkham S, Sheehan JK, Knight D, Richardson PS, Thornton DJ (2002) Heterogeneity of airways mucus: Variations in the amounts and glycoforms of the major oligomeric mucins MUC5AC and MUC5B. Biochemical Journal 361: 537-546.

Kreyling WG, Semmler-Behnke M, Möller W (2006) Ultrafine particle - Lung interactions: Does size matter? Journal of Aerosol Medicine: Deposition, Clearance, and Effects in the Lung 19: 74-83.

Laemmli UK (1970) Cleavage of structural proteins during the assembly of the head of bacteriophage T4. Nature 227: 680-685.

Lai SK, O'Hanlon DE, Harrold S, Man ST, Wang YY, Cone R, Hanes J (2007) Rapid transport of large polymeric nanoparticles in fresh undiluted human mucus. Proceedings of the National Academy of Sciences of the United States of America 104: 1482-1487.

Ledowski T, Manopas A, Lauer S (2008) Bronchial mucus transport velocity in patients receiving desflurane and fentanyl vs. sevoflurane and fentanyl. European Journal of Anaesthesiology 25: 752-755.

Ledowski T, Paech MJ, Patel B, Schug SA (2006) Bronchial mucus transport velocity in patients receiving propofol and remifentanil versus sevoflurane and remifentanil anesthesia. Anesthesia and Analgesia 102: 1427-1430.

Lehr CM (2000) Lectin-mediated drug delivery: The second generation of bioadhesives. Journal of Controlled Release 65: 19-29.

Leikauf G, Yeates DB, Wales KA (1981) Effects of sulfuric acid aerosol on respiratory mechanics and mucociliary particle clearance in healthy nonsmoking adults. American Industrial Hygiene Association Journal 42: 273-282.

Lethem MI (1993) The role of tracheobronchial mucus in drug administration to the airways. Advanced Drug Delivery Reviews 11: 271-298.

Lillehoj EP, Kim KC (2002) Airway mucus: Its components and function. Archives of Pharmacal Research 25: 770-780.

Loebau J, Rumphorst A, Galla K, Seeger S, Wolfrum K (1996) Adsorption of alkyl-trichlorosilanes on glass and silicon: A comparative study using sum-frequency spectroscopy and XPS. Thin Solid Films 289: 272-281.

Lu D, Hickey AJ (2007) Pulmonary vaccine delivery. Expert Review of Vaccines 6: 213-226.

Marttin E, Schipper NGM, Coos Verhoef J, Merkus FWHM (1998) Nasal mucociliary clearance as a factor in nasal drug delivery. Advanced Drug Delivery Reviews 29: 13-38.

Matsui H, Randell SH, Peretti SW, Davis CW, Boucher RC (1998) Coordinated clearance of periciliary liquid and mucus from airway surfaces. Journal of Clinical Investigation 102: 1125-1131.

Merkus P, Romeijn SG, Coos Verhoef J, Merkus FWHM, Schouwenburg PF (2001) Classification of cilio-inhibiting effects of nasal drugs. Laryngoscope 111: 595-602.

Metwalli E, Haines D, Becker O, Conzone S, Pantano CG (2006) Surface characterizations of mono-, di-, and tri-aminosilane treated glass substrates. Journal of Colloid and Interface Science 298: 825-831.

Moeller W, Haeußinger K, Kreyling WG, Scheuch G (2005) Particle clearance from the human respiratory tract. Atemwegs- und Lungenkrankheiten 31: 342-351.

Möller W, Häußinger K, Winkler-Heil R, Stahlhofen W, Meyer T, Hofmann W, Heyder J (2004) Mucociliary and long-term particle clearance in the airways of healthy nonsmoker subjects. Journal of Applied Physiology 97: 2200-2206.

Mudge J (1778) A radical and expeditious cure for a recent catarrhous cough. Allen, London, pp 1-252.

Mussatto DJ, Garrard CS, Lourenco RV (1988) The effect of inhaled histamine on human tracheal mucus velocity and bronchial mucociliary clearance. American Review of Respiratory Disease 138: 775-779.

Nafee N, Taetz S, Schneider M, Schaefer UF, Lehr CM (2007) Chitosan-coated PLGA nanoparticles for DNA/RNA delivery: effect of the formulation parameters on complexation and transfection of antisense oligonucleotides. Nanomedicine: Nanotechnology, Biology, and Medicine 3: 173-183.

NCRP (1997) Deposition, Retention and Dosimetry of Inhaled Radioactive Substances. NCRP Report No. 125

Neuss S, Apel C, Buttler P, Denecke B, Dhanasingh A, Ding X, Grafahrend D, Groger A, Hemmrich K, Herr A, Jahnen-Dechent W, Mastitskaya S, Perez-Bouza A, Rosewick S, Salber J, Woeltje M, Zenke M (2008) Assessment of stem cell/biomaterial combinations for stem cell-based tissue engineering. Biomaterials 29: 302-313.

Oberdörster G, Oberdörster E, Oberdörster J (2005) Nanotoxicology: An emerging discipline evolving from studies of ultrafine particles. Environmental Health Perspectives 113: 823-839.

Peters A, Veronesi B, Calderon-Garciduenas L, Gehr P, Chen LC, Geiser M, Reed W, Rothen-Rutishauser B, Schuerch S, Schulz H (2006) Translocation and potential neurological effects of fine and ultrafine particles a critical update. Particle and Fibre Toxicology 3

Pitcairn G, Reader S, Pavia D, Newman S (2005) Deposition of corticosteroid aerosol in the human lung by Respimat® Soft Mist™ inhaler compared to deposition by metered dose inhaler or by Turbuhaler® dry powder inhaler. Journal of Aerosol Medicine: Deposition, Clearance, and Effects in the Lung 18: 264-272.

Prophet EB, Mills B, Arrington JB, Sobin LH (1994) Laboratory Methods in Histotechnology. Armed Forces Insitute of Pathology, Washington (DC): American Registry of Pathology, pp 149-174.

Rabea EI, Badawy MET, Stevens CV, Smagghe G, Steurbaut W (2003) Chitosan as antimicrobial agent: Applications and mode of action. Biomacromolecules 4: 1457-1465.

Ravi Kumar MNV, Bakowsky U, Lehr CM (2004) Preparation and characterization of cationic PLGA nanospheres as DNA carriers. Biomaterials 25: 1771-1777.

Rubin BK (1988) Immotile cilia syndrome (primary ciliary dyskinesia) and inflammatory lung disease. Clinics in Chest Medicine 9: 657-668.

Rubin BK, Cheeseman CI, Gourishankar S, King M (1992) Is there a seasonal variation in mucus transport and nutrient absorption in the leopard frog? Canadian Journal of Physiology and Pharmacology 70: 442-446.

Rubin BK, Ramirez O, King M (1990) Mucus-depleted frog palate as a model for the study of mucociliary clearance. Journal of Applied Physiology 69: 424-429.

Russel WMS, Burch RL (1959) The Principles of Humane Experimental Techniques. Methuen, London.

Rytting E, Nguyen J, Wang X, Kissel T (2008) Biodegradable polymeric nanocarriers for pulmonary drug delivery. Expert Opinion on Drug Delivery 5: 629-639.

Sakagami M (2006) *In vivo*, *in vitro* and *ex vivo* models to assess pulmonary absorption and disposition of inhaled therapeutics for systemic delivery. Advanced Drug Delivery Reviews 58: 1030-1060.

Salathe M (2002) Effects of ß-agonists on airway epithelial cells. Journal of Allergy and Clinical Immunology 110

Sanders M (2007) Inhalation therapy: An historical review. Primary Care Respiratory Journal 16: 71-81.

Satir P, Christensen ST (2007) Overview of structure and function of mammalian cilia. Annual Review of Physiology, vol 69, pp 377-400.

Scheuch G, Fischer A (2008) Improved entry into the airways. Manufacturing Chemist 79: 39-40.

Scheuch G, Gebhart J, Heigwer G, Stahlhofen W (1989) New device for human inhalation studies with small aerosol boluses. Journal of Aerosol Science 20: 1293-1296.

Scheuch G, Siekmeier R (2007) Novel approaches to enhance pulmonary delivery of proteins and peptides. Journal of Physiology and Pharmacology 58: 615-625.

Scheuch G, Stahlhofen W (1987) Particle deposition of inhaled aerosol boluses in the upper human airways. Journal of Aerosol Science 18

Scheuch G, Zimlich WC, Siekmeier R (2007) Biophysical Parameters Determining Pulmonary Drug Delivery. In: Bechthold-Peters K, Luessen H (eds) Pulmoary Drug Delivery: Basiscs, Applications, and Opportunities for Small Molecules and Biopharmaceutics Editio Cantor Verlag, Aulendorf, pp 46-54.

Schurch S, Gehr P, Im Hof V, Geiser M, Green F (1990) Surfactant displaces particles toward the epithelium in airways and alveoli. Respiration Physiology 80: 17-32.

Selting K, Waldrep JC, Reinero C, Branson K, Gustafson D, Kim DY, Henry C, Owen N, Madsen R, Dhand R (2008) Feasibility and Safety of Targeted Cisplatin Delivery to a Select Lung Lobe in Dogs via the AeroProbe® Intracorporeal Nebulization Catheter. 21: 255-268.

Serra-Batlles J, Plaza V, Badiola C, Morejon E, Bardagi S, Brotons B, Cabello F, Castillo JA, Hermida JA, Lopez-Vinas A, Marin JM, Tabar A (2002) Patient perception and acceptability of multidose dry powder inhalers: A randomized crossover comparison of Diskus/Accuhaler with Turbuhaler. Journal of Aerosol Medicine: Deposition, Clearance, and Effects in the Lung 15: 59-64.

Shah AJ, Donovan MD (2007a) Formulating gels for decreased mucociliary transport using rheologic properties: Polyacrylic acids. AAPS PharmSciTech 8

Shah AJ, Donovan MD (2007b) Rheological characterization of neutral and anionic polysaccharides with reduced mucociliary transport rates. AAPS PharmSciTech 8: 32.

Sibille Y, Reynolds HY (1990) Macrophages and polymorphonuclear neutrophils in lung defense and injury. American Review of Respiratory Disease 141: 471-501.

Sleigh MA, Blake JR, Liron N (1988) The propulsion of mucus by cilia. American Review of Respiratory Disease 137: 726-741.

Smith PK, Krohn RI, Hermanson GT (1985) Measurement of protein using bicinchoninic acid. Analytical Biochemistry 150: 76-85.

Sogias IA, Williams AC, Khutoryanskiy VV (2008) Why is chitosan mucoadhesive? Biomacromolecules 9: 1837-1842.

Stahlhofen W, Gebhart J, Rudolf G, Scheuch G, Philipson K Clearance from the human airways of particles of different sizes deposited from inhaled aerosol boli 1986, pp 192-196.

Stahlhofen W, Koebrich R, Rudolf G, Scheuch G (1990) Short-term and long-term clearance of particles from the upper human respiratory tract as function of particle size. Journal of Aerosol Science 21: 407-410.

Thornton DJ, Rousseau K, McGuckin MA (2008) Structure and function of the polymeric mucins in airways mucus. Annual Review of Physiology, vol 70, pp 459-486.

Toomes H, Vogt-Moykopf I, Heller WD, Ostertag H (1981) Measurement of mucociliary clearance in smokers and nonsmokers using a bronchoscopic video-technical method. Lung 159: 27-34.

Van De Donk HJM, Zuidema J, Merkus FWHM (1982) Correlation between the sensitivity of the ciliary beat frequency of human adenoid tissue and chicken embryo tracheas for some drugs. Rhinology 20: 81-87.

Verdugo P (1990) Goblet cells secretion and mucogenesis. Annual Review of Physiology 52: 157-176.

Wang X, Xie X, Cai C, Rytting E, Steele T, Kissel T (2008) Biodegradable Branched Polyesters Poly(vinyl sulfonate-covinyl alcohol)-graft-Poly(D,L-lactic-coglycolic acid) as a Negatively-charged Polyelectrolyte Platform for Drug Delivery: Synthesis and Characterization. Macromolecules 41: 2791-2799.

Weibel ER (1979) Morphometry of the human lung: The state of the art after two decades. Clinical Respiratory Physiology 15: 999-1013.

Weiss B, Schaefer UF, Zapp J, Lamprecht A, Stallmach A, Lehr CM (2006) Nanoparticles made of fluorescence-labelled poly(L-lactide-co-glycolide): Preparation, stability, and biocompatibility. Journal of Nanoscience and Nanotechnology 6: 3048-3056.

Welch MJ, Nelson HS, Shapiro G, Bensch GW, Sokol WN, Smith JA, Parasuraman BM (2004) Comparison of patient preference and ease of teaching inhaler technique for Pulmicort Turbuhaler® versus pressurized metered-dose inhalers. Journal of Aerosol Medicine: Deposition, Clearance, and Effects in the Lung 17: 129-139.

WHO (2008) The top 20 causes of death in 2030. In: (WHO) WHO (ed) World Health Statistics 2008, pp 1-112.

Wills PJ, Suarez MJG, Rutman A, Wilson R, Cole PJ (1995) The ciliary transportability of sputum is slow on the mucus-depleted bovine trachea. American Journal of Respiratory and Critical Care Medicine 151: 1255-1258.

Wright JR (2004) Host defense functions of pulmonary surfactant. Biology of the Neonate 85: 326-332.

Yeates DB, Gerrity TR, Garrard CS (1982) Characteristics of tracheobronchial deposition and clearance in man. Annals of Occupational Hygiene 26: 245-257.

Curriculum Vitae

personal information

name	Andreas Michael Henning
date of birth	December 22nd, 1977
place of birth	Tuebingen, Germany

doctoral thesis

2005 – 2008	Biopharmaceutics and Pharmaceutical Technology, Saarland University, Saarbruecken, Germany

diploma thesis

2005	Biopharmaceutics and Pharmaceutical Technology, Saarland University, Saarbruecken, Germany "*Influence of different commonly employed human skin preparation techniques on the results of in vitro skin diffusion experiments"*

undergraduate study

1999 – 2003	Pharmaceutical studies Eberhard Karls University, Tuebingen, Germany Pharmaceutical State Examination in November 2003 Certification as Pharmacist in December 2004

military service

1997 – 1998	German Airforce Commandership, Messtetten

professional experience and teaching

2001	Teaching Assistant, *Practical Training in Analytical Chemistry*, Department of Medical Chemistry, Eberhard Karls University
2002	Research assistant, *Semi-quantitative isolation of boswellic acids*, Department of Pharmacology, Eberhard Karls University
2005 - 2006	Teaching Assistant, *Seminars and Supervision of the Practical Training in Pharmaceutical Technology*, Saarland University
2006 - 2008	Head Assistant, *Seminars and Supervision of the Advanced Exercises in Pharmaceutical Technology*, Saarland University
2006 and 2008	Lecturer and Lab Course Supervisor, *International Conference and Workshop on Biological Barriers and Nano-medicine: Advanced Drug Delivery and Predictive non vivo Testing*, Saarland University

Publication List

A) Scientific Publications

Henning A., Schneider M., Nafee N., Rytting E., Kissel T., Grafahrend D., Klee D., Lehr C.-M. (2009): Influence of particle size and surface properties on mucociliary clearance from the airways. *Journal of Controlled Release*, to be submitted.

Bur M., **Henning A.**, Schneider M., Lehr C.-M. (2009): Inhalative Nano-medicine. *Inhalation Toxicology*, in progress.

Henning A., Schaefer U.F., Neumann D. (2008): Potential pitfalls in skin permeation experiments: Influence of experimental factors and subsequent data evaluation. *European Journal of Pharmaceutics and Biopharmaceutics*, DOI: 10.1016/j. ejpb.2008.07.016, in print.

Henning A., Schneider M., Bur M., Blank F., Gehr P., Lehr C.-M. (2008): Embryonic chicken trachea as a new in vitro model for the investigation of mucociliary particle clearance in the airways. *AAPS PharmSciTech*, 9(2):521-527.

Henning A., Neumann D., Kostka K.H., Lehr C.-M., Schaefer U. (2008): Influence of human skin specimen consisting of different skin layers on the results of in vitro skin diffusion experiments. *Skin Pharmacology and Physiology*, 21:81-88.

Hansen S., **Henning A.**, Naegel A., Heisig M., Wittum G., Neumann D., Kostka K.H., Zbytovska J., Lehr C.-M., Schaefer U.F. (2008): In-silico model of skin penetration based on experimentally determined input parameters Part I: Experimental determination of partition and diffusion coefficients. *European Journal of Pharmaceutics and Biopharmaceutics*, 68(2):352-367.

Schneider M., **Henning A.**, Wahl B., Daum N., Lehr C.-M., Interaction of Nanoparticulate Matter with Biological Barriers. *Proceedings of the International School on Advanced Material Science and Technology*, September 4-7, 2007, pp. 25-36, Ancona, Italy.

Bur M., **Henning A.,** Lehr C.-M., Alveolar epithelial cell culture – a useful tool in aerosol drug delivery research, Respiratory Drug delivery X; Biological, Pharmaceutical, Clinical, and Regulatory Issues Relating to Optimized drug Delivery by Aerosol, April 23-27, 2006, Boca Raton Resort and Club, Florida, USA.

B) Book Chapters

Henning A., Hein S., Schneider M., Bur M., Lehr C.-M. (2009): Aerosol Delivery: Inhaling Medicines. In: Handbook of Experimental Pharmacology: Novel Drug Delivery Approaches; Eds. Hofmann F., Schaefer-Korting M.S., Springer, New York, USA, in print.

Hein S., **Henning A.**, Bur M., Schneider M., Lehr C.-M. (2009): Particulate Carriers for Pulmonary Drug Delivery. In: Particle-Lung Interactions, 2nd Edition; Eds. Gehr P., Blank F., Muehlfeld C., Rothen-Rutishauser B., Informa Healthcare, London, Great Britain, in print.

C) Awards

Lecture award for best oral presentation (1st price) from the Controlled Release Society Germany (CRS Germany). *Annual Meeting and Exposition of the CRS Germany*, Braunschweig, Germany, March 2008.

D) Contribution to Scientific Conferences

Podium:

Henning A., Schneider M., Bur M., Lehr C.-M.: Is particle size a decisive parameter for nanoparticle clearance from the airways? *Meeting and Exposition of the Controlled Release Society Germany*, Braunschweig, Germany, March 2008.

Posters:

Henning A., Schneider M., Bur M., Lehr C.-M.: Decisive parameters for particle clearance from the airways: Particle size vs. mucoadhesion. *Annual Meeting and Exposition of the Controlled Release Society*, New York, USA, June 2008.

Henning A., Schneider M., Bur M., Lehr C.-M.: Physico-chemical determinants for nanoparticle clearance from the airways? *Pulmonet International Symposium on "Secretion and transport in normal and diseased pulmonary epithelia"*, Saarbruecken, Germany, March 2008.

Henning A., Schneider M., Bur M., Lehr C.-M.: Influence of various drugs on particle clearance utilizing embryonic chicken trachea, a new tool for the investigation of mucociliary clearance in vitro. *XII. German Meeting on Aerosol Therapy*, Marburg, Germany, November 2007.

Henning A., Schneider M., Bur M., Lehr C.-M.: Embryonic chicken trachea as a new in vitro model to investigate mucociliary particle clearance. *16th Congress of the International Society of Aerosols in Medicine (ISAM)*, Tours, France, June 2007.

Henning A., Schneider M., Bur M., Lehr C.-M.: Embryonic Chicken Trachea as a new in vitro model to investigate mucociliary particle clearance: Influence of temperature and humidity. *Alternative Test Methods in Inhalation Toxicology (ATMIT)*, Federal Institute for Risk Assessment, Berlin, Germany, May 2007.

Bur M., **Henning A.**, Lehr C.-M.: Alveolar epithelial cell culture: a useful tool in aerosol drug delivery research. *Respiratory Drug Delivery X*; Biological, Pharmaceutical, Clinical, and Regulatory Issues Relating to Optimized Drug Delivery by Aerosols; Boca Raton Resort and Club, Florida, USA, April 2006.

Henning A., Neumann D., Lehr C.-M., Schaefer U.F.: In vitro drug penetration across different human skin preparations: hydrophilic vs. lipophilic donor medium. *International Conference and Workshop on Biological Barriers and Nanomedicine: Advanced Drug Delivery and Predictive non vivo Testing Technologies*, Saarbruecken, Germany, March 2006.

Henning A., Netzlaff F., Meiers P., Lehr C.-M., Schaefer U.: Direct in vitro comparison of human Stratum corneum, Epidermis, Dermatomized skin, Dermis and Full-thickness skin permeability. *Annual Meeting and Exposition of the American Association of Pharmaceutical Scientists (AAPS)*, Nashville, USA, November 2005.

Henning A., Netzlaff F., Meiers P., Lehr C.-M., Schaefer U.: Influence of different human skin preparations on the results of in vitro skin permeation experiments. *Annual Meeting and Exposition of the German Pharmaceutical Society (DPhG)*, Mainz, Germany, March 2005.

Acknowledgements

First and foremost, I would like to thank Professor Dr. Claus-Michael Lehr for the possibility to join his working group, and for his scientific as well as squarely advice during my Ph.D. studies.

Furthermore, I am greatly indebted to Junior Professor Dr. Marc Schneider for co-supervising this work, and for his endurance in a great many discussions on methodology and technical details of the microscope set-up.

Many thanks to Dr. Ulrich Schaefer, Dr. Dirk Neumann, and Dr. Michael Bur for their friendly support during my time at the 'Lehr lab', and for their helpful discussions and comments on technical as well as administrative issues.

I must thank Professor Dr. Peter Gehr for giving me the opportunity to realize the SEM and TEM studies on chicken embryo trachea. These studies were of highest importance to characterize the morphological constitution of the ECT model.

The Germany Federal Ministry of Education and Research (BMBF) and the NanoInhale project managers at Boehringer Ingelheim, namely Dr. Michael Krueger and Dr. Régis Cartier, are thanked for the generous funding and determined handling of the overall project.

For a really good working atmosphere, for their companionship, and for the good collaboration - which is not a matter of course - my special gratitude goes to all colleagues from the working group, and especially to: Barbara, Christine, Davide, Eva, Frank, Haukon, Katharina, Marco, Nico, Noah, Sebastian, Steffi, and Stephan.

I would also like to thank the technical staff for their encouragement and persistent help in i.a. histochemical methods, analytics, and for monitoring all the required instruments during the last 4 years in the ‘Lehr lab’: Leon Muijs, Peter Meiers, and Petra Koenig.

Finally and most importantly, I must thank my parents, my brothers Martin and Matthias, and my girlfriend Anna, for believing in me, for listening, and for supporting whatever I do. Thank you!!!

During my studies I have had the chance to interact with many interesting and highly remarkable people. To everyone who is not mentioned here, please forgive me and to all of you my deep respect, appreciation and sincere gratitude.